LBL-6756
c.1

Presented at the VIIth International
Conference on High-Energy Physics and
Nuclear Structure, Zurich, Switzerland,
August 29 - September 2, 1977

INTERACTION OF NUCLEI AT HIGH ENERGIES

Herbert Steiner

August 1977

Prepared for the U. S. Department of Energy
under Contract W-7405-ENG-48

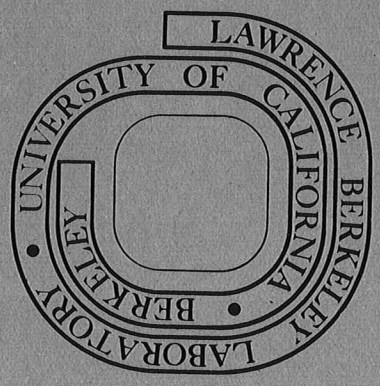

LBL-6756
c.1

INTERACTION OF NUCLEI AT HIGH ENERGIES

Herbert Steiner
Department of Physics and Lawrence Berkeley Laboratory
University of California, Berkeley, CA 94720

I. Introduction

In the last five years there has been a sharp increase in activity, both experimental and theoretical, in the study of collisions between energetic nuclei. Here I would like to review briefly the present status of this field of research with particular emphasis on recent developments. Because of time limitations I will have to omit a number of relevant and interesting topics such as hadron-nucleus interactions at very high (20 - 400 GeV) energies. Fortunately there are several recent reviews on this subject[1,2,3]. In any case I would like to apologize in advance to all those who may feel slighted (or offended) by my remarks.

I think it is important at the outset to spend just a little time discussing the physics behind these experiments. Are we really exploring basically new domains of physics, are we getting new insights into existing questions of interest, or are we (as some of my colleagues have suggested) simply making our lives difficult by studying particle interactions in a messy and complicated environment? For each of these questions the answer is probably yes, and I leave it to the interested spectator to classify the results presented here accordingly.

The title of this Conference "High Energy Physics and Nuclear Structure" very aptly characterizes the physics which is involved. The high energies allow us to study the nuclear structure of the individual participating nuclei especially in peripheral processes where we can kinematically separate fragmentation processes associated with the target from those coming from the projectile. The high energies are also important in that they make possible the study of relativistic components of nucleon wave functions. Experiments with energetic nuclei have been undertaken to determine cluster structure, density fluctuations, high internal momentum components of the constituent nucleons, and it may not be too far fetched to hope that in such high energy reactions we may even learn something about the quark structure of nuclei. In central collisions high energies are needed if we are to produce nuclear matter under extreme conditions of temperature, density and pressure, which in turn could conceivably lead to such new phenomena as density isomers or even new stable forms of nuclear matter[4], pion condensates[5], shock waves[6], and other exotic processes. The distinction between central and peripheral processes is of course not clear cut, especially for the experimentalists. Operationally such interactions are characterized on the basis of the multiplicity of the emitted fragments (including pions) the presence or absence of fast forward moving particles, the transverse momentum distributions, and various correlations between the detected particles. The use of nuclei gives us new degrees of freedom in studying high energy interaction mechanisms. At high enough energies (e.g. $\geq$ FNAL, SPS) it may well become possible to study the space-time development of particle production. Already nuclei have been used to investigate the interaction between resonances and nucleons.

With the vast amounts of new data it becomes imperative to find means to present results as simply and as clearly as possible. In this respect the traditional double differential cross section as a function of angle and energy is usually not very appropriate. Rather, Lorentz invariant cross sections as a function of Lorentz invariant variables often greatly facilitate the comparison of experiments with each other and with the predictions of theoretical models.

II. Single Particle Inclusive Spectra

Perhaps the most popular experimental activity has been the measurement of single particle inclusive spectra. The reasons are simple: the experiments tend to be relatively straight-forward and the theoretical interpretations may not be completely impossible. Among the contributions to this conference are some 9 papers dealing with this subject. More new results can be found in preprint form and in published articles [7 - 15]. The objectives of such studies is varied, ranging from attempts to determine the dominant interaction mechanisms to getting direct information about nuclear structure.

Much interest has focused on establishing the relation between hadron-hadron, hadron-nucleus and nucleus-nucleus collisions to see what features are common to these reactions. The emphasis here is mostly on

high-energy processes with the aim of determining the essential parameters which control the asymptotic behavior. The concepts of limiting fragmentation, scaling and factorization as applied to nuclear reactions have been and continue to be subjected to many tests. Of great interest also is the study of high $p_\perp$ phenomena. Here the intent is to probe more deeply into the short distance structure of nuclear matter. Of course interaction mechanisms are closely related to the structure of the interacting systems and a topic which has received much attention is to what extent several nucleons participate jointly in these reactions. The term cumulativity has been introduced by the Dubna group[16] to characterize such communal happenings. The effects of high internal momentum components of constituents in nuclei and multiple hadronic scattering also play important roles in many of these reactions and it is not easy to untangle and isolate unambiguosly the various contributions to the observed spectra.

I would like to separate the nuclear structure aspects of these single particle inclusive experiments into two categories: (1) "Normal" or "Traditional" topics such as for example the cluster structure in nuclei, the density distributions of the constituent neutrons and protons, and (2) "Abnormal" or "New" topics related to the behavior of nuclear matter under extreme conditions of temperature, pressure and density. The interpretation of these experiments is unfortunately still very model dependent and definitive conclusions are consequently not yet possible. Still a great deal of activity has been and continues to be dedicated to this problem, both experimentally and theoretically.

Single particle inclusive spectra have been measured over a wide range of kinematic variables, and for a variety of projectiles and targets. At the high energies considered here the experiments themselves fall naturally into two main groups - one involving the measurement of relatively low energy fragments associated with the target while the other focuses on highly relativistic forward moving fragments originating in the projectile. The rapidity diagram in Fig. 1 schematically illustrates these kinematic domains, and the fact that the underlying physics is the same. The shaded regions are of particular interest because there the rapidities of the emitted fragments can and often do exceed the limits attainable in free nucleon-nucleon collisions and in such cases the nuclear wave functions must play an important role.

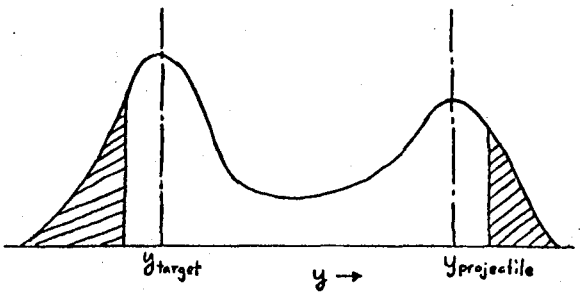

Fig. 1

Schematic illustration of the rapidity distribution of fragments in nucleon-nucleus collisions.

Speculations about the detailed mechanisms responsible for the production of particles into these shaded kinematic regions have been plentiful, and I will have more to say about these later (see THEORETICAL MODELS).

The intermediate region of rapidity is not devoid of interest, and in particular proponents of "nuclear fireballs"[17] have tried to find structures in the rapidity distributions which can be associated with such objects.

II.A. Some Selected Experiments

II.A.1 Projectile fragmentation

In an experiment at the LBL Bevalac, Anderson et al.[8] have made a systematic study of single particle inclusive spectra resulting from the collisions of relativistic light nuclei with nuclear targets. The following reactions were studied:

Projectile		Target		Fragment
p, d, α, ^{12}C	+	CH_2, C, Cu, Pb	→	$\pi^\pm$, p, d, ^3H, ^3He, α, ⋮ + X

p_{in} = 0.93 GeV/c Nucleon $\quad 0.25 \leq \frac{p}{z} \leq 9$ GeV/c

1.75 GeV/c Nucleon $\quad 0^o \leq \theta \leq 12^o$

2.88 GeV/c Nucleon $\quad 0 \leq \frac{p_\perp}{z} \leq .8$ GeV/c

A double focusing spectrometer was used in conjunction with a series of scintillation counters and multiwire proportional

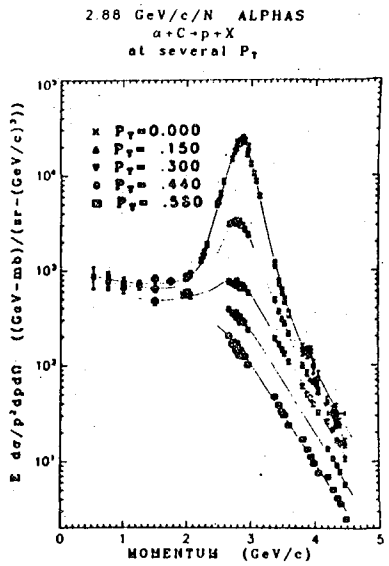

Fig. 2

Momentum distributions of protons at several values of transverse momentum for the reaction 2.88 GeV/c/N α + C → p + X. Curves are hand-drawn merely to guide the eye. The data points for a given P_T do not always join continuously since the value of P_T is not exactly constant.

chambers. Fig. 2 gives an example of the data obtained for the case α + C → p + X. Similar spectra were obtained for other projectiles, targets, and fragments at each incident momentum. As can be seen from Fig. 2 the emphasis in this experiment was on the projectile fragmentation region although the no-man's land between target and projectile momentum was also covered.

Some typical results are shown in Fig. 3 to Fig. 9 . Already in Fig. 2 we see that the momentum distributions in the lab system are not symmetric about the peak position. Nor do they become symmetric when they are transformed to the projectile's rest frame as can be seen in Fig. 3, the difference being due at least in part to the longitudinal momentum transfer between projectile and the target. Furthermore the region to the left of the peak in Fig. 2 (and the corresponding region labelled $p_L^{proj} < 0$ in Fig. 3 is just where target and projectile fragmentations ultimately have to merge in contrast to the region to the right of the peak in Fig. 2 which must fall to zero because of energy-momentum conservation. In Fig. 4 comparison is made between the

$p_L^{proj} > 0$

distribution for $p_\perp = 0$ and the $p_\perp$ distribution at

$p_L^{proj} = 0$.

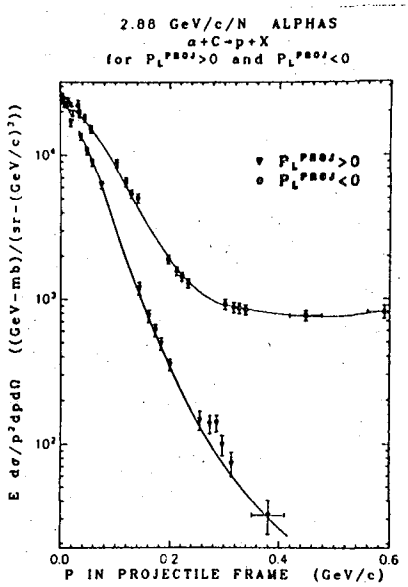

Fig. 3

Momentum distribution in the projectile frame for proton produced at $P_T = 0$ in the reaction 1.75 GeV/c/N α + C → p + X. The distribution is clearly not isotropic in the projectile frame.

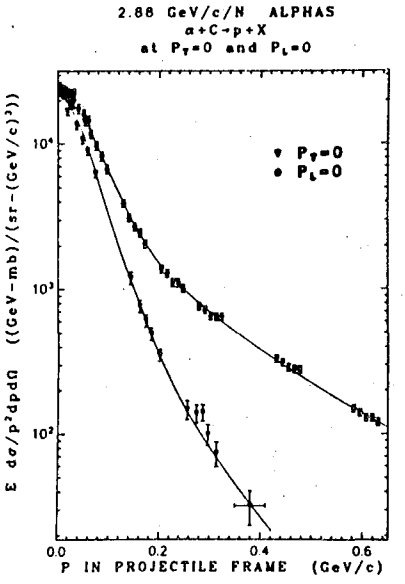

Fig. 4

Distributions in projectile frame longitudinal momentum

(p_L^{proj}) for $P_T = 0$, and in

P_T for $p_L^{proj} = 0$

for protons in the reaction 2.88 GeV/c/N α + C → p + X. Isotropy is again violated.

We see that the $p_\perp$ distribution is much broader. In this case the transverse momentum transfer is the culprit. In fact, whereas the width of the

$$p_L^{proj} > 0$$

is dominantly determined by the corresponding internal momentum distribution of the constituents in the projectile, the transverse momentum distribution can trace its origins both to the internal momentum and to the characteristic 200 - 300 MeV/c transverse momentum transfer which is typical of hadronic scattering processes. Although I have shown only one example of this effect here, it is quite general, at least for light nuclei, and should be kept in mind when one tries to extract internal momentum distributions from fragmentation data. It is perhaps also worth pointing out that by the time $p^{proj} \approx 0.4$ GeV/c is reached the $p_\perp$ and $p_\parallel$ distributions differ by an order of magnitude.

The $p_\perp$ distribution of the protons in the reaction $\alpha + C \rightarrow p + X$ is shown in Fig. 5 for the case

$$p_\parallel^{proj} = 0$$

for three incident momenta. We see that these distributions are independent of projectile energy to an accuracy of $\lesssim 10$ %.

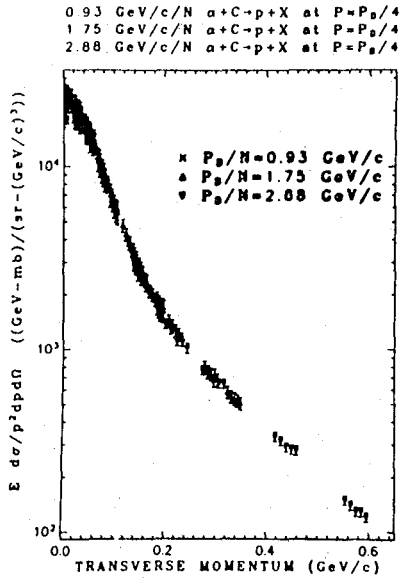

Fig. 5

Transverse momentum distributions of projectile velocity of protons for three energies of incident alphas. The distribution is approximately limiting.

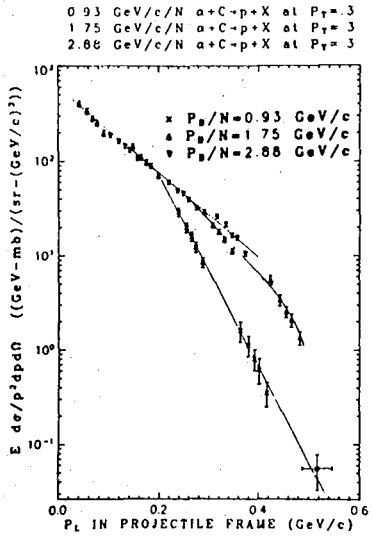

Fig. 6

Projectile frame longitudinal momentum distributions of protons at $p_T = 0.3$ GeV/c, for three energies of incident alpha projectiles on a carbon target. The limiting behavior breaks down at high momentum.

Similar distributions for other fragments also seem to be "universal". On the other hand the

$$p_L^{proj} > 0$$

distributions at fixed $p_\perp$ do not scale at high p, perhaps because of kinematical constraints imposed by energy-momentum conservation (see Fig. 6). The $p_\perp$ distributions for $\alpha + T \rightarrow \alpha + X$ show a very characteristic diffraction structure when the α-fragment satisfies elastic kinematics in contrast to the $p_\perp$ behavior for non-elastic scattering as can be seen in Fig. 7. The $x_R = \frac{p^*}{(p^*)_{max}}$ distribution of protons in the reaction $\alpha + C \rightarrow p + X$ for 1.75 GeV/c/Nucleon α projectiles is shown in Fig. 8 for two cases:

$p_\perp = 0$ and $p_\perp = 0.3$ GeV/c. Upon closer inspection one notes that the peak shifts to slightly lower values of x as $p_\perp$ increases. The fall-off in the region $.8 \lesssim x \lesssim 1.0$ is noticeably less steep for the $p_\perp = 0.3$ GeV/c case than for $p_\perp = 0$. The curves are fits to the form $(1-x)^g$ suggested by the model of Schmidt and Blankenbecler. The reason for showing this figure is to prepare the model builders for the deluge - there is a lot more data of this general type now available and my experimental friends hope thereby to sharply curtail the room in

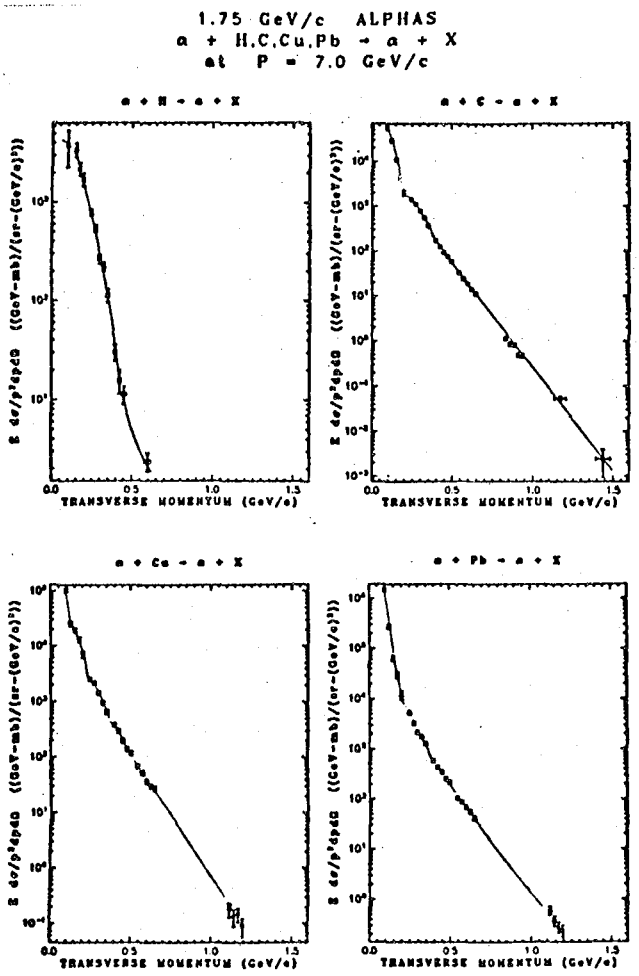

Fig. 7

Transverse momentum distributions of alpha particles at the incident momentum for 1.75 GeV/c/N alpha beams incident on H, C, Cu, and Pb targets. Diffraction structure is quite evident.

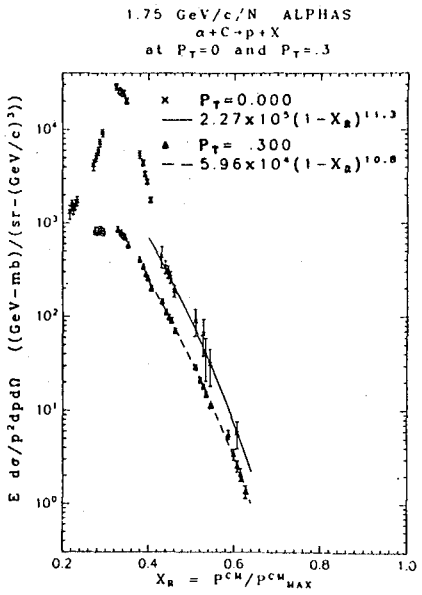

Fig. 8

Distribution in X_R for protons at P_T = 0, and 0.3 GeV/c for the reaction 1.75 GeV/c/N α + C → p + X. The curves are fits to the data points through which they pass for the parameterization $(1-X_R)^N$.

which their theoretical colleagues can maneuver. The A_T dependence of the various fragmentation processes depends mainly on the fragment momentum, $p_\perp$ and to a lesser extent on fragment type. The power n in a fit of the cross section to A^n is shown in Fig. 9a and Fig. 9b for various p_F, $p_\perp$ and fragment types. As can be seen the value of n increases markedly for very low fragment momenta as would be expected if these fragments are associated with the target. The increase of n with increasing $p_\perp$ is reminiscent of the $p_\perp$ behavior in hadron-nucleus collisions at very high energies[18].

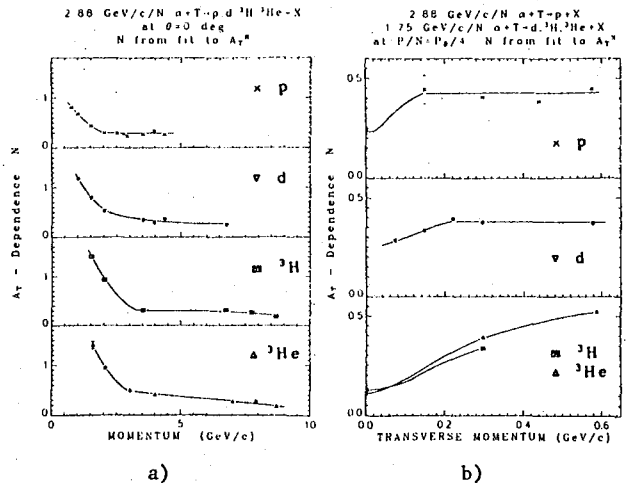

Fig. 9a, Fig. 9b

Results of fitting the target dependence of the production of p, d, ^{3}H, and ^{3}He by 2.88 GeV/c/N alpha particles on C, Cu, and Pb targets. Fig. 9a shows N as a function of momentum at θ = 0° and Fig. 9b shows N as a function of p_T for projectile velocity fragments.

II.A.2 Target fragmentation

An experiment with emphasis on the target fragmentation and central regions has been reported by J. Gosset et al.[12]. The reactions studied were

Projectile		Target		Fragment		
^{4}He	+	Al	→	p	+ X	
^{20}Ne		U		d		
				⋮		
				light nuclei		

K.E. = 0.25 GeV/n $30 \leq T_F \leq 150$ MeV/N

0.40 $25^o \leq \theta \leq 150^o$(lab)

2.1

Scintillators and solid state detectors deployed around the target were used to identify the fragments and to measure their energies and angles. An example of the light fragment cross sections for 0.4 GeV/N (p = 0.93 GeV/c/N) ^{20}Ne + U is shown in Fig. 10. The 90° cross sections correspond to the

$p_{\parallel}^{proj} = 0$ situation of the previous experiment. In Fig. 11 we see a comparison of the 90° ^{3}He cross sections when ^{20}Ne at various energies collide with Uranium. In contrast to Anderson et al.[8] the cross sections differ markedly in magnitude and to a lesser extent in shape at the various bombarding energies. It should be kept in mind that here we are looking at the fragmentation of Uranium whereas before we looked at fragments from α-particles; furthermore, the $p_\perp$ intervals are different in the two experiments. In the present case for example there are ^{3}He fragments having kinetic energies of 100 MeV/nucleon which corresponds to a momentum of 1.3 GeV/c.

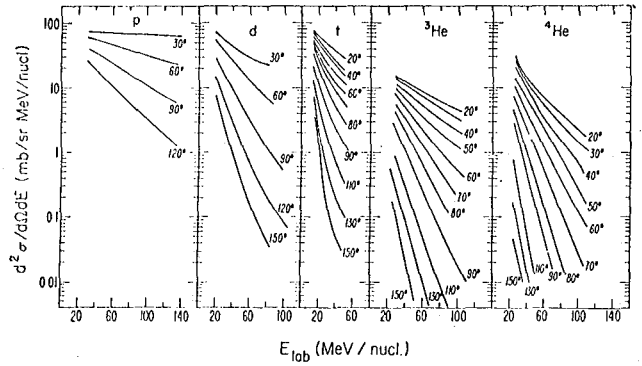

Fig. 10

Energy distributions at various angles of p, d, ^{3}He and ^{4}He for 0.4 GeV/N, Ne on U.

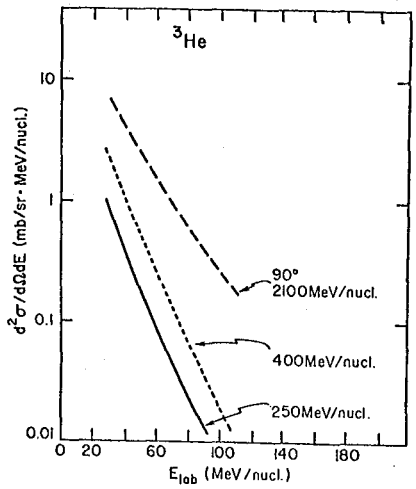

Fig. 11

Energy distributions of ^{3}He observed at 90° (lab) in reactions of ^{20}Ne on U at three different bombarding energies.

If we restrict ourselves to ^{3}He fragments having kinetic energies between 30 and 50 MeV/nucleon it turns out that the angular distributions differ only by an overall normalization factor of 10 for 0.4 GeV/N ^{4}He and 0.4 GeV/N ^{20}Ne projectiles. At other bombarding energies the shapes of the angular distributions are different (see Fig. 12).

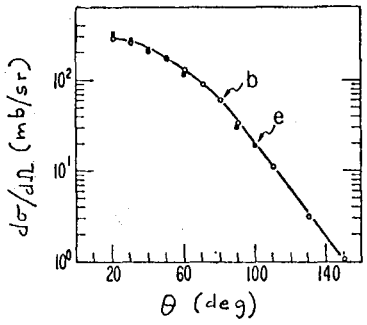

Fig. 12

Angular distributions of ^{3}He fragments with energy window 30 - 50 MeV/N; (b) indicates the case of 400 MeV/N Ne on U and (e) indicates the case of 0.4 GeV/N α on U raised by a factor of 10.

The invariant cross section as a function of momentum at 90° is shown in Fig. 13 for fragments produced when 400 MeV/N ^{20}Ne interact with uranium. The similarity of the slopes [(140 MeV/c)$^{-1}$] for the various fragments is striking.

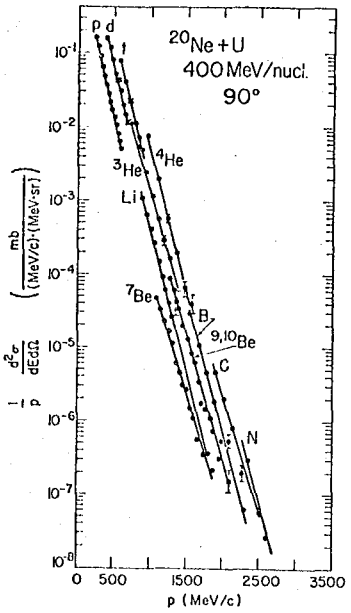

Fig. 13

Invariant cross section versus momentum p for all fragments measured at 90° from 400 MeV/N ^{20}Ne on U.

Other qualitative features of the data include the following:

(1) All light fragment energy spectra are smooth except for an "evaporation peak" at very low energies.

(2) The most neutron deficient isotopes exhibit spectra with a relatively higher cross section in the high energy tail.

(3) The slope of the fragment spectra in the intermediate energy range gets steeper with increasing detection angle. Angular distributions are forward peaked.

(4) The double differential cross sections at 30° are approximately independent of the incident energy. At larger angles the yield increases and the slope decreases with increasing bombarding energy.

(5) The slope of the fragment spectra in energy/nucleon at a given angle gets steeper with increase in fragment mass.

(6) The total yields of light fragments fall off with increase in mass. At energies of 30 - 50 MeV/nucleon cluster emission comprises a significant fraction (about 50 %) of the total baryonic cross section. Towards higher energies protons become predominant.

(7) Increasing the projectile mass at a fixed incident energy per nucleon leads to a small increase in the cross section for low energy fragments but to a larger increase at high fragment energies, especially for the heavier clusters.

(8) In Ne bombardment of U and Al targets besides the difference in overall absolute cross section, one finds for Al a depletion of cross section at back angles.

II.A.3 Large angle fragmentation

In another experiment with relativistic heavy ions at Berkeley Nagamiya et al.[15] measured pion, proton and light fragment spectra at large angles. A magnetic spectrometer together with multiwire proportional chambers and counters were used to study the following reactions:

Projectile	Target	Fragment
C, Ne	C, NaF, Cu, Pb	$\pi^{\pm}$, p, d, ...

800 MeV/nucleon

$50 \leq T_F \leq 2000$ MeV

$15^{\circ} \leq \theta_L \leq 145^{\circ}$

Typical inclusive spectra for protons and pions are shown in Fig. 14 and Fig. 15.

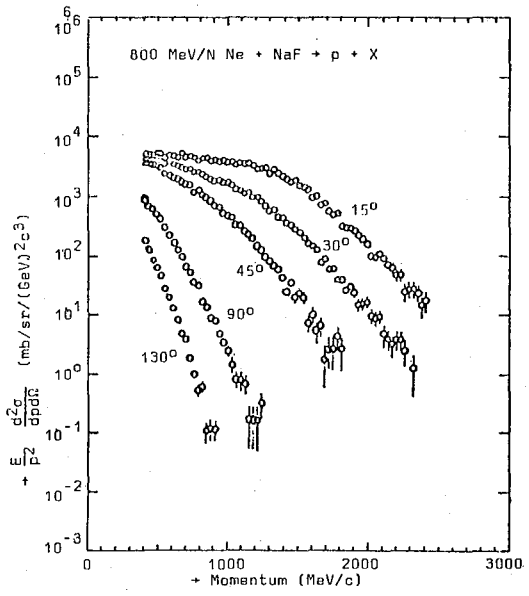

Fig. 14

Inclusive proton spectra observed at various laboratory angles from 800 MeV/N Ne on NaF. Invariant cross sections are plotted versus laboratory momentum.

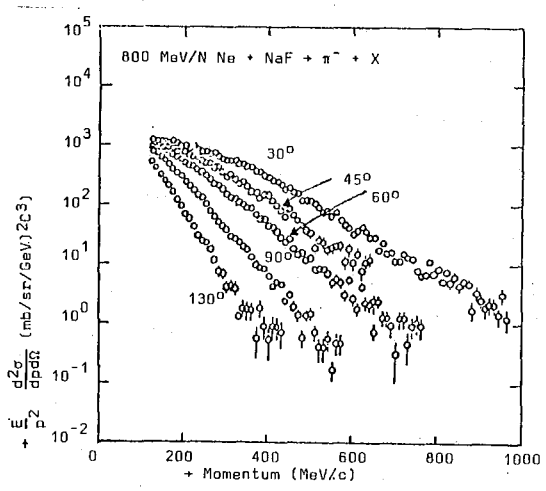

Fig. 15

Inclusive pion spectra observed at various laboratory angles from 800 MeV/N Ne on NaF.

Contour plots of the inclusive proton cross sections in the ($p_\perp$, y) plane show that the double peak structure characteristic of low $p_\perp$ processes at high energy gradually merges into a single broad distribution (Fig. 16). When we plot the proton energy distribution for the case when for a given invariant cross section the protons have their maximum transverse momentum, it turns out that the distribution is exponential with a characteristic fall-off constant of about 70 MeV (see Fig. 17). The A_T dependence is very dependent on angle (or equivalently on $p_\perp$) as shown in Fig. 18 and Fig. 19. For protons, at very large angles, the power n in A_T^n exceeds 1, again very reminiscent of the high $p_\perp$ p-nucleus observations at FNAL[18].

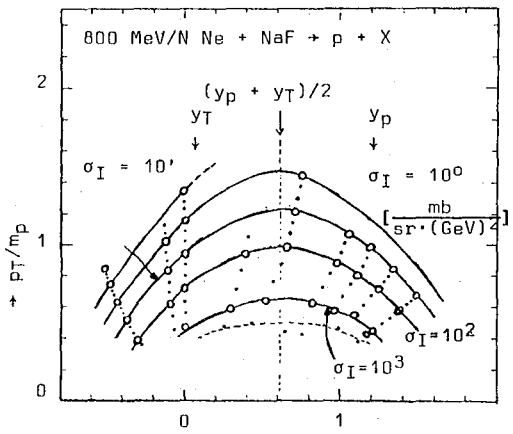

Fig. 16

Contours of constant invariant cross section in the plane of rapidity (y) and p_T/m_p.

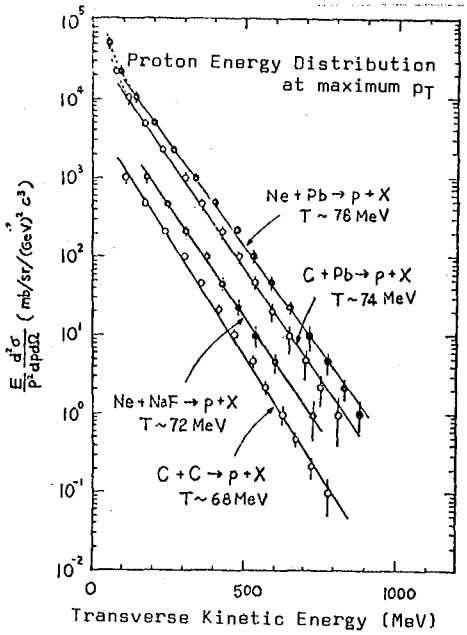

Fig. 17

Energy distributions of protons having maximum p_T (for given invariant cross section) for various reactions. Incident energies of C and Ne are 800 MeV/N.

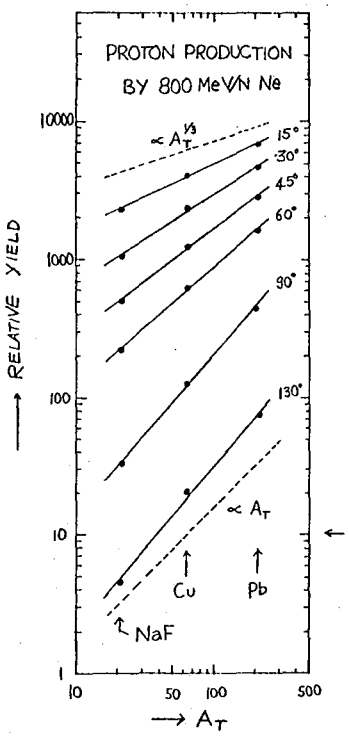

Fig. 18

Target mass dependence of proton production by 800 MeV/N Ne.

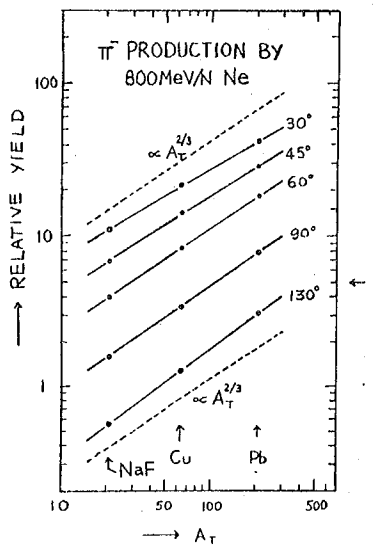

Fig. 19

Target mass dependence of pion production by 800 MeV/N Ne.

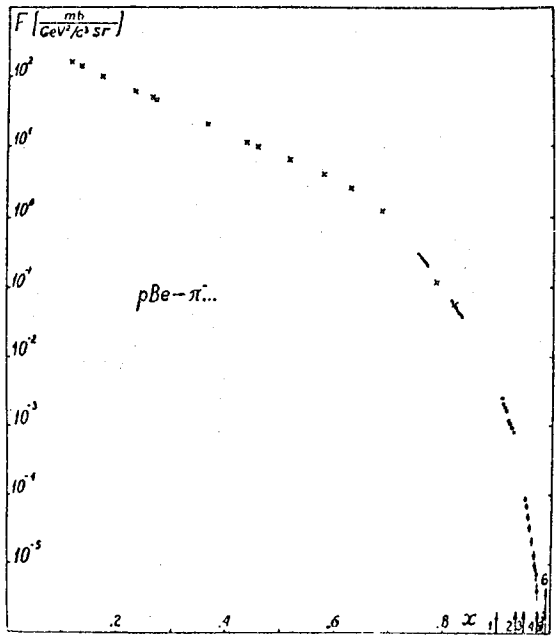

Fig. 20

Invariant cross section versus

$x \equiv p_{\parallel}^{lab}/p_{\parallel max}^{lab}$ for p + Be → π⁻ + X reaction

at 8.8 GeV/c bombarding momentum and at θlab = 62 mrad. ● shows the data by Beyukov et al. and x taken from Barabash et al.

II.A.4. Production of pions and protons with maximum momenta

In an experiment performed at ITEP Bayukov et al.[19] studied the production of pions with maximum momenta in proton-nucleus interactions at 8.8 GeV/c. A magnetic spectrometer selected negative particles emitted at 62 mrad, and scintillation counters were used as detectors. An example of the invariant cross section as a function of

$$x = \frac{p_{\parallel}^{LAB}}{(p_{\parallel}^{LAB})_{max}}$$

is shown in Fig. 20 for p + Be → π⁻ + x. Similar spectra were obtained with Al, Cu, and Au targets. To compare the invariant cross section, F_A, for pion production from Al, Cu, and Au to that of Be, Bayukov et al. calculated the ratio

$$R_{A/Be}(x) = \frac{\rho_A(x)}{\rho_{Be}(x)}$$

where

$$\rho_A(x) = \frac{F_A(x)}{\sigma_{pA}^{in}} .$$

A plot of $R_{A/Be}(x)$ is shown in Fig. 21. They suggest that the sharp rise in $R_{A/Be}$ near x = 1 may be due to higher internal momentum components in the heavier targets

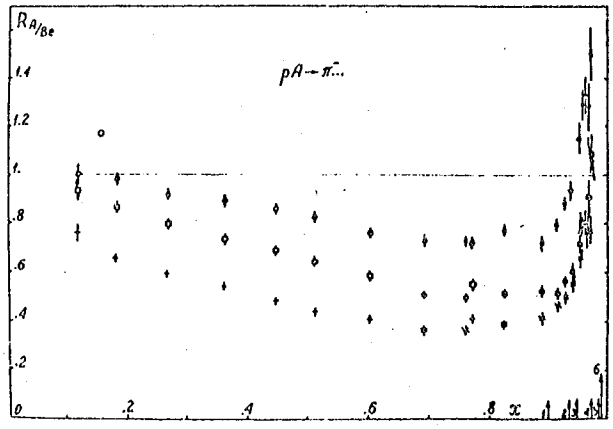

Fig. 21

Ratio $R_{A/Be} = \rho_A/\rho_{Be}$ as a function of x where $\rho_A = F_A/\sigma_{pA}^{in}$. ● - Al, ■ - Cu, x,◊ - Al, □ - Cu, † - Ta.

compared to those in Be. However, in their paper they state that they use the approximation

$$p_{\parallel max} = E_p - m_p$$

which is exact in the limit $A = \infty$ and $\theta = 0^{o}$. Because the invariant cross section is falling so steeply near $x = 1$ even the very small A dependent correction to their approximation for

$$(p_{\parallel})_{max}$$

is important and tends to supress the rise shown in Fig. 21. For the ratio $R_{A/Al}(x)$ they see no significant rise, but then the approximation $A = \infty$ is much better for Al and heavier nuclei than for Be. They also state that their observations are qualitatively consistent with production from a separately moving nucleon in the nucleus, although quantitative comparisons await detailed model calculations.

In a related experiment Belikov et al.[20] measured π^- and proton generation at 188 mrad in proton-nucleus interactions at 9 GeV/c. They find that the shapes of the invariant cross sections, F(x), for pions and protons are similar and both extend beyond the kinematic region for scattering from a nucleon at rest (see Fig. 22). In the investigated region of x and $p_\perp$ the invariant functions $F(x, p_\perp)$ do not depend on the initial momentum for $p_o \geq 9$ GeV/c to an accuracy of $\sim$ 15 %. The ratio $R_{Cu/Be}(x, p_\perp)$ for pions increases with increasing $p_\perp$ at fixed x for $0.3 \leq x \leq 0.6$. As shown in Fig.23/24 for the case of protons both the ratios $R_{A/Be}(x, p_\perp)$ and $R_{A/Al}$ increase with increasing x at the fixed laboratory angle of 188 mrad, the increase being greatest near the kinematical limit.

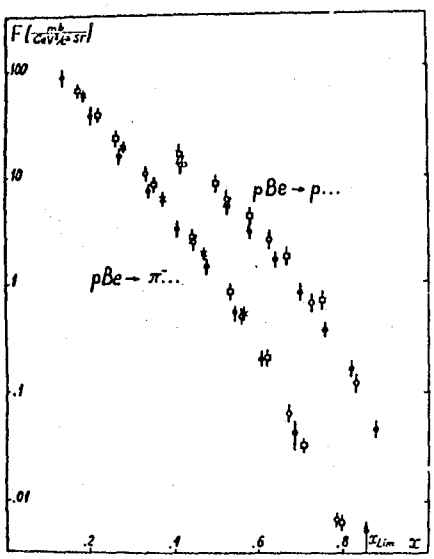

Fig. 22

Invariant cross section

$$F \equiv \frac{E}{p^2}\frac{d^2\sigma}{dp d\Omega} \quad \text{versus x.}$$

● - p_o = 9 GeV/c by Bayukov et al.,
x - p_o = 12.4 GeV/c by Barabash et al.,
0 - p_o = 19.2 GeV/c by Allaby et al.,
□ - p_o = 24 GeV/c by Eichten et al.

The laboratory angle is 188 mrad at p_o = 9 GeV/c and for higher energy the data at corresponding p_T are plotted.

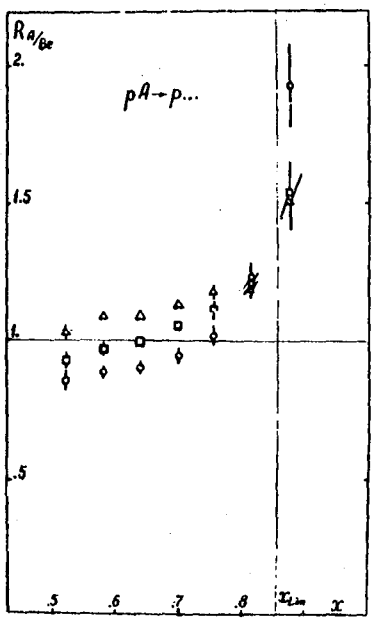

Fig. 23

Ratios $R_{A/Be}$ for A = Al (Δ), A = Cu (□) and A = Au (o).

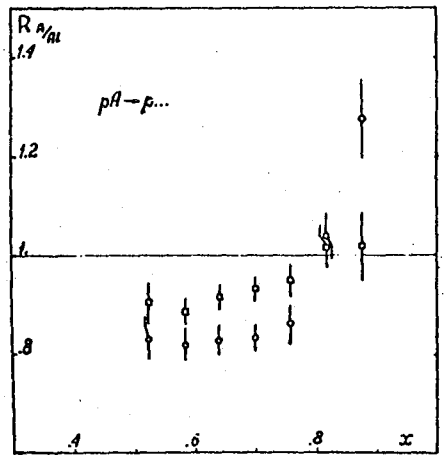

Fig. 24

Ratio $R_{A/Al}$ for A = Cu (□) and A = Au (o).

The mechanism responsible for the rise near $x = x_{lim}$ is not yet established. Among the possibilities suggested by the authors are interaction of the incident proton with a cluster heavier than a nucleon, differences in the Fermi-motion in various nuclei, or multiple scattering effects.

II.A.5. Recent single particle results from Dubna

The study of single particle spectra is part of an active continuing research program involving high energy interactions between nuclei at the JINR, Dubna[21]. For example new results are available on the production of particles at angles of 80° to 180° in proton and deuterium collisions at a beam momentum of 8.6 GeV/c. An example of these data is shown in Fig. 25 from Baldin[21] which shows the angular distribution of fragments having $p_F/Z = 0.64$ GeV/c. This figure shows that care must be taken in extrapolating data to 180°. Baldin[21] states that the simplest existing models of the cumulative effect, which have been used successfully by Dubna groups to fit a number of other experiments, are not yet able to explain the detailed structure observed here. On the other hand he also says unequivocally in referring to experiments in kinematical regions forbidden for nucleon-nucleon collisions that "The discovered A dependences and scale invariance exclude completely the possibility of explaining the relevant experimental data by means of Fermi motion and are in agreement with predictions based on the hypothesis about the existence of the cumulative effect".

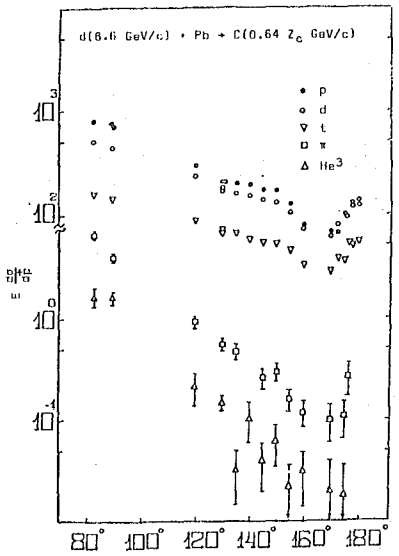

Fig. 25

Angular distribution of fragments C in deuterium lead collisions.

II.A.6. Backward proton production by protons, deuterons and α particles

In an experiment at SREL Brody et al.[22] measured backward proton production in the collision of protons (600 MeV), deuterons (361 MeV), and alpha particles (722 MeV) with various targets. A magnetic spectrometer and counters were used. An example of their results is shown in Fig. 26. The high energy protons emitted at 180° fall into the kinematic domain indicated by the left-most shaded region of Fig. 1. This kind of experiment, which has also been very actively pursued by some of the members of the same group at LAMPF as well as by several groups in Dubna and elsewhere, continues to stimulate a lot of speculation about the underlying mechanisms. Brody et al. get good fits to their data by assuming that for Fermi-momentum components between $0.4 \leq p_F \leq 1.5$ GeV/c there is an exponential tail to the internal momentum distribution, F(k), which can be approximated by the form

$$F(k) = \frac{e^{-k/k_o}}{k} .$$

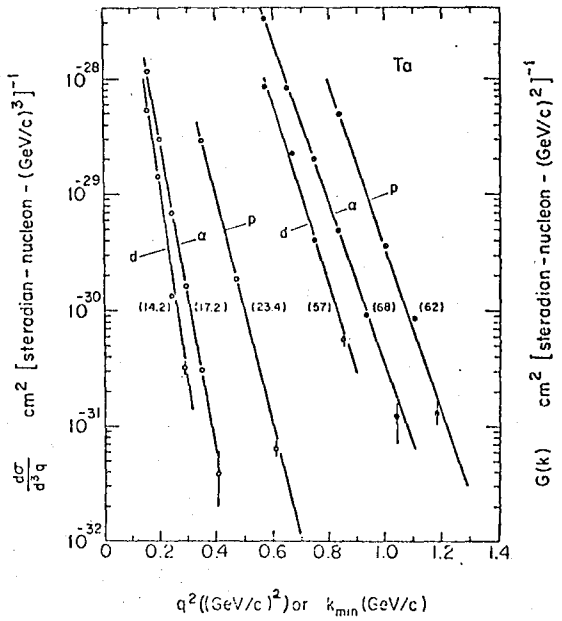

Fig. 26

Differential cross sections/nucleon versus q^2 (left hand curves) and G (k_{min}) versus k_{min} (right hand curves) for Ta target. Numbers in parenthesis are α^{-1} from fit to

$$\frac{d\sigma}{dq^2} = B \exp.\left(-\alpha \frac{q^2}{2m_p}\right)$$

and k_o from fits to G (k_{min}) = b exp.$\left(-\frac{k}{k_o}\right)$.

From their experimental fits they obtain k_0 (Li) $\simeq$ 85 MeV/c, k_0 (C) $\simeq$ 70 MeV/c, and k_0 (Ta) $\simeq$ 62 MeV/c pretty much independent of the type of incident particle.

Frankel[23] has made a detailed analysis of a large amount of fragmentation data in this general kinematic domain, and concludes that the data can be well fit by such a model which he calls "quasi-two body scaling". As we have already seen the Dubna group on the other hand prefer to interprete their results in terms of the "cumulative effect", i.e., the interaction of the projectile with a small cluster of nucleons inside the nucleus, and also get very good agreement with the experimental data. It seems to me that these seemingly different approaches may not be so different after all, and that they may represent two complementary descriptions of the same basic process. Since we have been led rather naturally into a discussion of models let us look at some of them in more detail.

II.B. The Models

The models are not quite as plentiful as the data points - but almost - as a quick glimpse of recent publications, preprints and Conference Contributions will show. Just as in the case of the experiments I will confine this discussion to some typical examples. No attempt will be made to be complete; rather, I would like to focus on a few ideas which seem to me to be both interesting and representative of the various approaches used. I think it is fair to say that none of these theories, at least in their present incarnations, describe the data fully, but that certain simple ideas seem to work quite well in fitting sizeable amounts of data in specific kinematic domains. It is probably fair to say that theories attempting to describe peripheral processes are in better shape than those for central collisions. I will rather arbitrarily divide the approaches into the following four categories:

(1) Microscopic models - e.g. Glauber type models, cascades, interaction of constituents, multiple scattering, ...

(2) Cumulative effects - e.g. fluctuons, coherent clusters, coherent tubes, ...

(3) Macroscopic - e.g. hydrodynamic, thermodynamic, statistical, fireballs, ...

(4) Other - e.g. high internal momentum components, final state interactions, ...

II.B.1 Type (1) theories

My own personal favorite among the recently proposed models is an independent particle type model by Schmidt and Blankenbecler[24]. Consequently I will discuss it in somewhat greater detail than the others. It is a theoretical attempt to explain the fragmentation spectra observed in high energy nuclear collisions using a generalization of the relativistic hard-collision models of composite hadrons. Here the constituents are nucleons. The diagram in Fig. 27 forms the basis for the calculations.

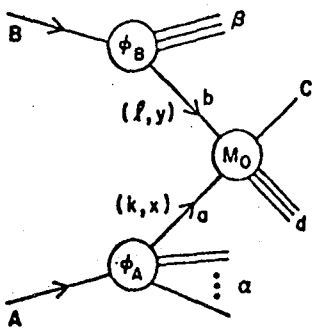

Fig. 27

The basic hard scattering model diagram to describe A + B → C + X.

The vertex functions ϕ are related directly to the distribution functions of constituent a in nucleus A, $G_{\frac{a}{A}}(x,\vec{k}_\perp)$.

Here x is a typical scaling variable, in this case defined to be the light cone scaling variable, which physically is related to the fractional momentum that particle a carries with respect to that of A, and $k_\perp$ is the transverse momentum. The actual calculations involve approximations which are most reasonable when the fragment has a momentum substantially different from either target or projectile; i.e. when it is in the shaded regions of Fig. 1. The emphasis is thus on the short distance behaviour of the nuclear wave function. Referring again to Fig. 27 the procedure is to take M_0 from experiment for the on-mass-shell case and then to extrapolate it to the off-shell case. Because at this stage of the calculations shadowing, rescattering and spin effects are neglected the theory is most applicable to the fragmentation of light nuclei. The invariant cross section,

$$R_C \equiv E_C \frac{d^3\sigma}{d^3p_C},$$

for producing fragment C in the process A + B → C + anything is written

$$R_c = \sum_{a,b} \int dx d^2k_\perp dy d^2\ell_\perp \times$$

$$\times G_{\frac{a}{A}}(x,\vec{k}_\perp)\, G_{\frac{b}{B}}(y,\vec{\ell}_\perp)\, r(s',s,x,y) \times$$

$$\times \left[E_c \frac{d^3\sigma}{dp_c}(a+b\to c+d;\ s',t',u')\right]$$

Here, r (s',s,x,y) is a phase space factor ∿ 1. Blankenbecler and Schmidt use a relativistic, generalized Hulthen-type wave function and then show that for the shaded kinematic domains of Fig. 1

$$G(x,\vec{k}_\perp) \sim (1-x)^g \quad \text{for } k_\perp^2 \text{ small}$$

$$\sim (k_\perp^2)^{-g-1} \quad \text{as a function of } k_\perp^2 .$$

The power g depends on the nature of the interaction of the nucleons in the nucleus. They explicitly consider three cases:

(A) For a renormalizable interaction between constituents (e.g. vector exchange) g = 2A-3

(B) For a super-renormalizable theory (e.g. scalar exchange) g = 4A-5

(C) For a nucleon-nucleon interaction involving vector exchange with monopole form factors at each vertex (e.g. vector dominance models) g = 6A-7.

The G's play the central role in this description since they are the unknown quantities to be explicitly determined from experiment. Several general properties of these distribution functions can be stated:

(1) G is peaked at $k_\perp = 0$. In fact they expect

$G \propto e^{-R^2k_\perp^2}$

with $R \sim A^{1/3}$ for large A.

(2) G is peaked when x corresponds to the momentum configuration where the nucleons share equally the total momentum of the nucleus.

(3) g which controls both the x = 1 and large $k_\perp$ behaviour is easy to characterize in terms of the basic interaction and the number of constituents.

(4) $G(x \sim 1, \vec{k}_\perp)$ is new information which is not accessible to conventional nuclear theory.

In their original paper Schmidt & Blankenbecler compare their model to the experimental data of Papp et al.[7] and find impressive agreement in fitting to the observed shapes. Some of these predictions for the three types of constituent interactions mentioned before are listed below and compared to experiment in Fig. 28 to Fig. 32.

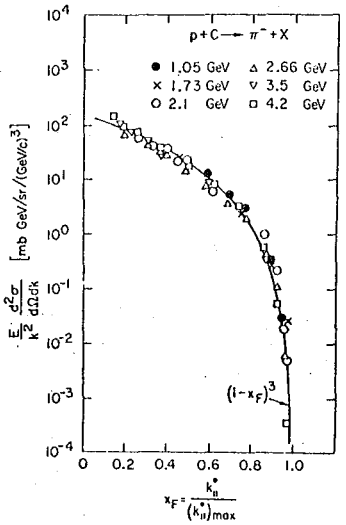

Fig. 28

The X_F spectrum compared to the carbon data illustrating scaling.

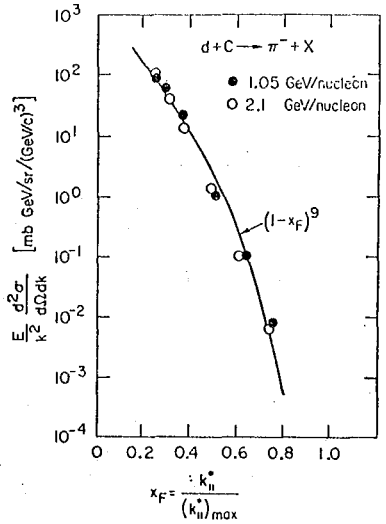

Fig. 29

The prediction by the vector dominance model (c) compared to the data by Papp et al. for a deuteron beam.

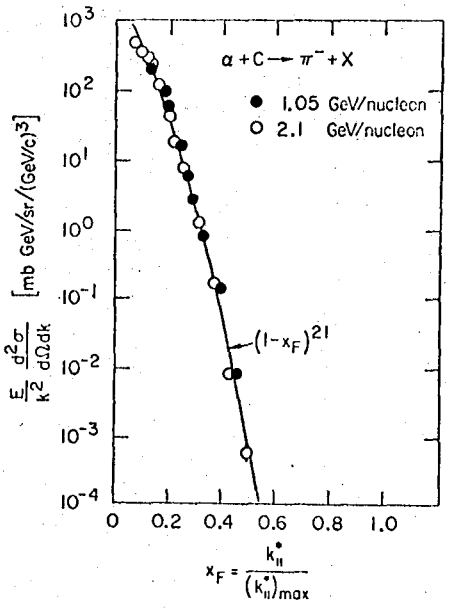

Fig. 30

The prediction by the vector dominance model (c) compared to the data by Papp et al. for an alpha particle beam.

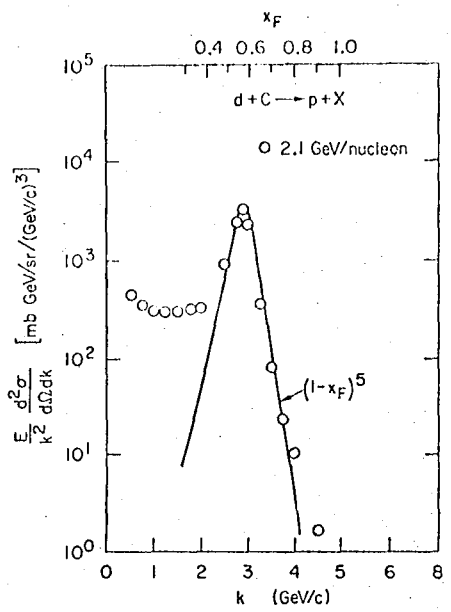

Fig. 31

The prediction by the vector dominance model (c) for inclusive protons from a deuteron beam. The full curve is a fit to the quasi elastic peak using the theory in the text by Schmidt and Blankenbecler.

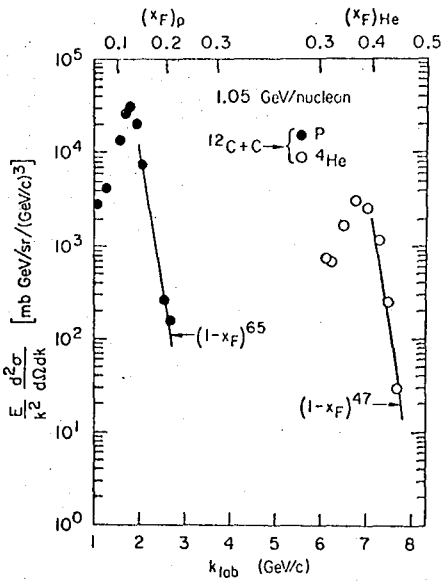

Fig. 32

Two inclusive processes for a carbon beam illustrating the counting rules and the positions of the quasi-elastic peaks.

Process	Forward $R_C \propto (1-x_F)^{n_i}$			Backward $R_C \propto (1+x_F)^{n_i}$			Fig.
	n_A	n_B	n_C	n_A	n_B	n_C	
p+C→π⁻	3	3	3	23	45	67	28
d+C→π⁻	5	7	9	25	47	69	29
α+C→π⁻	9	15	21	25	47	69	30
d+C→p	1	3	5	21	43	65	31
C+C→p	21	43	65	21	43	65	32
C+C→α	15	31	47	15	31	47	32

(R_C is the invariant cross section.)

Agreement of the model to the more extensive recent measurements of Anderson et al.[8] has been less impressive, as can be seen in Fig. 8. Actually reasonable fits to the form $(1-x)^n$ can be obtained for large enough x, but the exponent, n, at times differs markedly from the predictions of model C. Similar mixed successes occur when the theoretical predictions are compared to the data of Nagamiya et al.[5] Still I find the model quite compelling both from the point of view of the postulated mechanisms and its ability to fit data. Among the features of this model which seem to be of particular interest are:

(1) It is a relativistic formulation in terms of the structure functions $G(x,k_\perp)$ which can be obtained from experiment.

(2) The counting rules based on the short range N-N interaction determine the behaviour of the fragmentation cross section.

(3) Generally good agreement with experiment has been obtained for one simple model; i.e. vector exchange with monopole form factors at each vertex, which also agrees with other data.

(4) The vector exchange model with monopole form factors has the same counting rules as the quark dimensional counting model. This is perhaps surprising because the energies seem too low to excite the quark degrees of freedom.

(5) The power g is independent of energy.

(6) The model fits quasi-elastic scattering.

(7) The predictions for scattering at backward angles can be checked.

(8) The model allows one to describe a region of the wave function which cannot be described in non-relativistic theories.

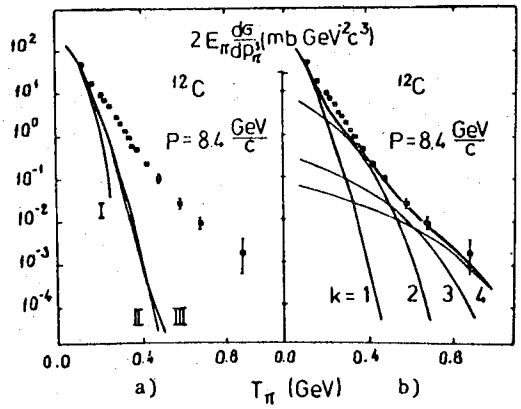

Fig. 33

a)
The calculation of the pion production invariant cross section on ^{12}C:
I the production on nucleons at rest,
II taking into account the Fermi motion,
III taking into account the relativistic effects;

b)
the contributions to the cross sections from separate fluctuons with mass M_k = km where k is the order of cumulativity.

II.B.2 Type (2) theories

A number of models based on variations of the cumulative effect have been proposed recently. For example Burov et al.[25] have speculated on the possible existence of fluctuons in nuclei and the role they might play in the production of particles into the shaded kinematic regions of Fig. 1. Basically a fluctuon is a localized ($\sim$ 0.5 - 0.7 fm) density fluctuation which can occur when more than one nucleon finds itself in a small volume. Burov et al. first show that the pion production cross sections of the Dubna group[26] cannot be explained with an independent particle model using normal Fermi-motion and taking into account relativistic effects of the nucleons in the nucleus. By invoking fluctuons they effectively increase the mass of the target and hence the energy available to produce pions. They use a simple form for the nuclear wave function to calculate the relative probability of finding k = 1,2,3,... nucleons inside a small volume of radius (r $\sim$ 0.5 - 0.7 fm). Here k is the order of cumulativity. The subsequent fits to the data are shown in Fig. 33. They then develop a microscopic theory of pion production from nuclei in which the fluctuons are the basic constituents. Their theory has obvious similarity to that of Schmidt and Blankenbecler. They

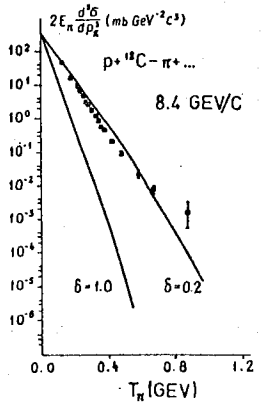

Fig. 34

The comparison with experiment of the pion production cross section on ^{12}C at δ = 0.2 and 1, where δ is a fitted parameter invoked in order to account for the non-asymptotic incoming energy.

too parametrize their structure functions of the fluctuons

$$G_{j/k}(x_k) \sim x_k^{\gamma_j(1)} (1-x_k)^{\gamma_j(2) + 6(k-1)},$$

where $x_k = p_j/p_{fl}$. Using this model they get good fits to the data for both pion and proton inclusive spectra (Fig. 34 and

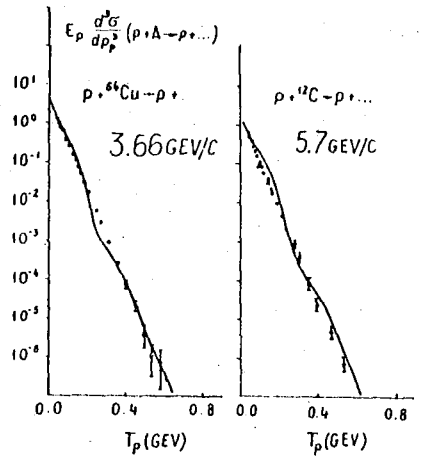

Fig. 35

Comparison of theoretical cross sections in the reactions of cumulative production of protons on nuclei with experiment.

Fig. 35). They conclude that the idea of nuclear fluctuations makes it possible to quantitatively understand the main regularities of inclusive spectra resulting from proton-nucleus collisions. In this approach the experiments yield information about the probabilities of finding nucleons in a small volume of the order of the nucleon-nucleon core, which is a slightly different way of saying that such experiments determine the small distance behavior of the nuclear wave function. They suggest that it would be of considerable interest for experimentalists to study processes on nuclei involving momentum transfers considerably larger (e.g. 7 - 10 fm^{-1}) than those investigated at present.

In another variant of the same general idea Fujita[27] introduces the concept of correlated clusters as a mechanism for the cumulative effect. The point here is that collisions sometimes take place from a more extended group of nucleons which stay as they are during fast collisions at high energies. He finds that clusters involving up to four nucleons are needed to fit the backward scattering data of Frankel et al.[28].

Coherent tubes[29] provide still another picture whereby several nucleons act jointly in producing particles and this model, too, has been successfully used to describe many of the general features of the data.

II.B.3 Type (3) theories

The third class of models has tended to be directed more toward a description of central processes than peripheral ones, although in principle such models should be applicable generally. The Hydrodynamic Calculations by Amsden et al.[32], and the Fireball model of Westfall et al.[17] are among several which have recently been used with mixed success to explain fragment spectra resulting from fast heavy ions on heavy nuclear targets. They seem to work best at the lower energies. In my opinion these models are still at a stage where their shortcomings in describing the observations outweigh their virtues.

II.B.4 Type (4) models

One idea, which has had considerable success in explaining the spectra of composite fragments, is that final state interactions between nucleons play an important role in the emission of hydrogen and helium isotopes. Gutbrod et al.[30] have been able to extend the original model of Butler and Pearson[31] to the production of various light isotopes in relativistic heavy ion collisions. They use the observed proton spectra to calculate the statistical probability of finding several nucleons in a small volume in momentum space, and this probability is then used to estimate the number of coalesced clusters which are formed. The model, with only one free parameter, has impressively described a large body of data. An example is shown in Fig. 36.

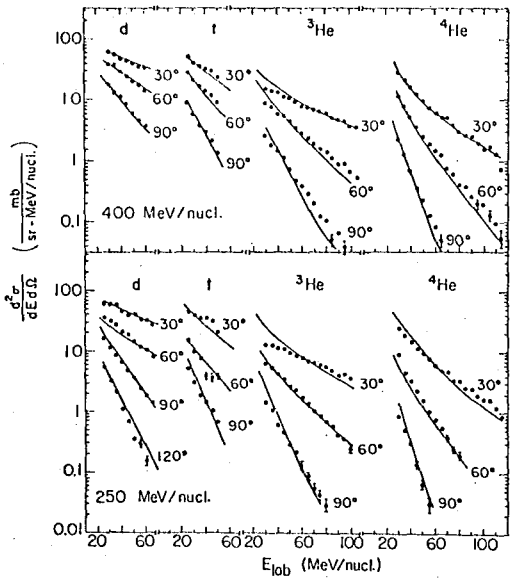

Fig. 36

Double differential cross sections for hydrogen and helium isotopes from ^{20}Ne on U compared with calculations (lines) using the coalescence formalism.

Another example of the final category of models involves the concept of "Quasi-Two Body Scaling" by Frankel[23]. His idea is to attribute the production of particles into the shaded regions of Fig. 1 to single collisions between the incident projectile and a constituent in the target having very high internal momentum. He postulates that above about p = 0.4 GeV the Fermi-momentum distribution has an exponential tail of the form

$$F(k) = \frac{e^{-k/k_o}}{k} \quad .$$

The phyiscal basis for this tail is not discussed, although it too must be related to the short distance behavior of the nuclear wave function. As the bombarding energy increases it becomes kinematically possible to investigate higher and higher internal momentum components. As stated in the discussion of the 180° production experiments this model has been quite successful in describing the general features of such data.

I hope that this short discussion of models has at least conveyed the idea that lots of ideas are being tried and that none of them yet fully describes the observations. It seems clear that there must be a close connection between many of these seemingly different approaches. More detailed measurements, especially those involving the energy and the A dependence of these reactions will be important in refining our theoretical understanding of such processes.

III. Multiparticle Final States

In interactions of protons with nuclei at very high energy the measurement of multiparticle final states has provided important information about the interaction mechanisms. Among the characteristic universal features of such studies are the observations that (1) the ratio

$$R = \frac{\langle n \rangle_{pA}}{\langle n \rangle_{pp}}$$

is a linear function of the parameter

$$\bar{\nu} = \frac{A\sigma_{pp}}{\sigma_{pA}}$$

($\bar{\nu}$ is a measure of the number of collisions in the nucleus), and (2) that the partial cross section for producing a certain multiplicity

$$\sigma_n = \frac{1}{\langle n \rangle} \psi \left(\frac{n}{\langle n \rangle}\right) \quad .$$

(KNO scaling.) (See Fig. 37 and Fig. 38.) In nucleus-nucleus collisions it is not yet clear how to generalize (1) although several suggestions based on such concepts as "wounded" nucleons[31], participants and spectators[34] have been postulated. The descriptions depend on the kinematical domains into which the observed particles are emitted. So far, KNO scaling seems to be satisfied in nucleus-nucleus collisions 21).

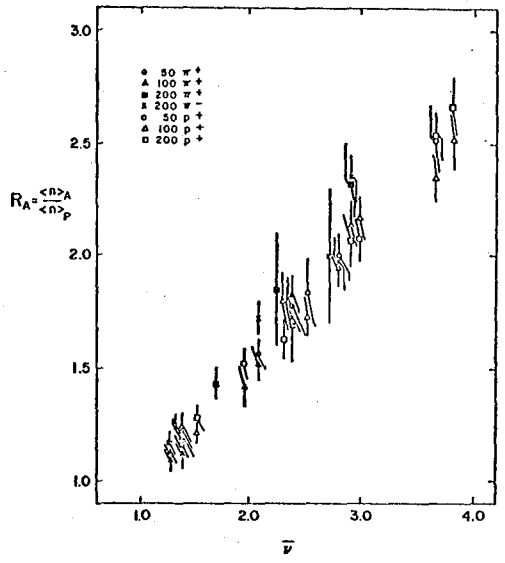

Fig. 37

Variation of R_A with $\bar{\nu}$. R_A is a measure of the multiplication of hadrons in the nucleus and $\bar{\nu}$ of the average thickness of the nucleus. Data are from Busza et al. $R_A \sim 1/2 + 1/2\ \bar{\nu}$ can be seen.

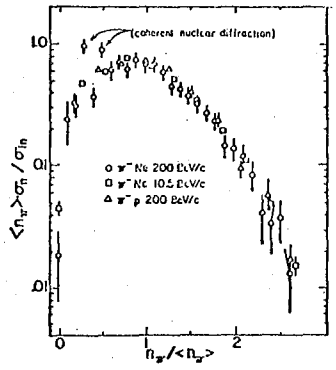

Fig. 38

Evidence for KNO scaling in hadron-nucleus collisions. Multiplicity distributions in π^--Ne collisions are plotted, using the data by Elliot et al.

Multiparticle final states have an important bearing on questions relating to the existence of shock phenomena, pion condensates, and other "exotic" processes. One of the major problems in this field is to know what to expect even if only "normal" processes take place. Up to now the various theoretical calculations disagree with each other and with experiment by factors 2 - 5 and consequently it has not yet been possible to arrive at definitive conclusions.

The present status of shocks seems to be that there is nothing shocking to report. The observation by Baumgardt et al.[6] of sharp peaks in the angular distribution of heavily ionizing particles emitted in high multiplicity events when various nuclear projectiles at various energies interact with AgCl are still tantalizing but have not been seen in other subsequent experiments[35,36]. In a contribution to this conference Toneev et al.[37] report that their analysis of the available data indicates that the formation of high density nuclear shock waves has not yet been proved experimentally.

III.A. Some Selected Experimental Results

III.A.1. Pion multiplicities at threshold

The subject of pion multiplicities in nucleus-nucleus collisions has stimulated both experimental and theoretical activity. For example in a recent paper McNulty et al.[38] report on an experiment to measure "threshold" pion production in the collision of 50 - 280 MeV/n Ne in emulsions. The pion identification is based on ionization. Their analysis leads them to conclude that (1) pions are emitted in 70 % of all interactions, (2) the average pion multiplicity per pion producing event is $\langle n_\pi \rangle = 2.8$ (although they do not state if this includes neutral pions), (3) the production of low energy pions is a very steep function of the energy of the Ne projectiles (see Fig. 39), (4) the observed energy spectrum of the pions peaks at about 100 MeV, although they state that pions with energies below 50 MeV would not be recognized. They then compare their results to an independent particle model calculation by Bertsch[39] and find disagreement. On the other hand the fact that they find reasonable agreement with the pion condensation model of Kitazoe et al.[40] leads them to state that their results "can be interpreted as evidence for pion condensation of the form described by Kitazoe and co-workers"[38]. It should be pointed out that their experimental

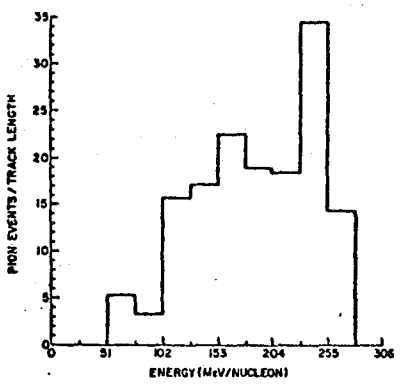

Fig. 39

Production of pions as a function of Ne energies.

technique does not insure unambiguous identification of pions. Any substantial misidentification could significantly affect the above-stated conclusion. In a brief comment at this conference B.Jakobsson[36] reported that his colleagues in Sweden see no pion production when 75 - 100 MeV ^{16}O nuclei interact in emulsions. Their results are shown in Fig. 40.

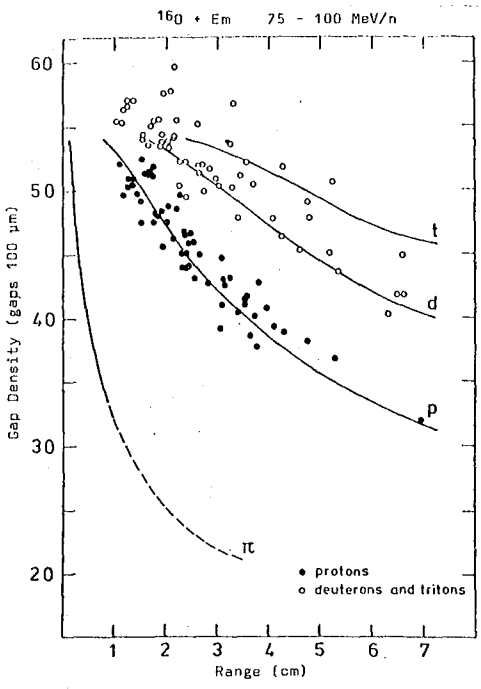

Fig. 40

Reaction products from the interaction of 75 - 100 MeV/n ^{16}O nuclei with emulsion; data by Jakobsson et al.[36]

III.A.2. Pion multiplicities at other energies

In an experiment in the LBL streamer chamber Fung et al.[41] have measured π^- production in relativistic heavy ion collisions. Projectiles of ^{12}C and ^{40}Ar at energies of 0.4 - 2.1 GeV/nucleon were incident on targets of LiH, NaF, BaI_2, and Pb_3O_4. Results on the average number of negative pions, $\langle N_\pi - \rangle$ and the ratio $\langle N_\pi - \rangle$ / $\langle N \rangle$ where $\langle N \rangle$ is the average number of charged fragments are shown in Table I. We see that this ratio rises sharply with increasing energy, but that it is roughly independent of projectile and target. These results are difficult to reconcile with those of McNulty et al. who claims to observe higher average multiplicities at lower energies compared to this experiment. An example of the angular and momentum distributions is shown in Fig. 41.

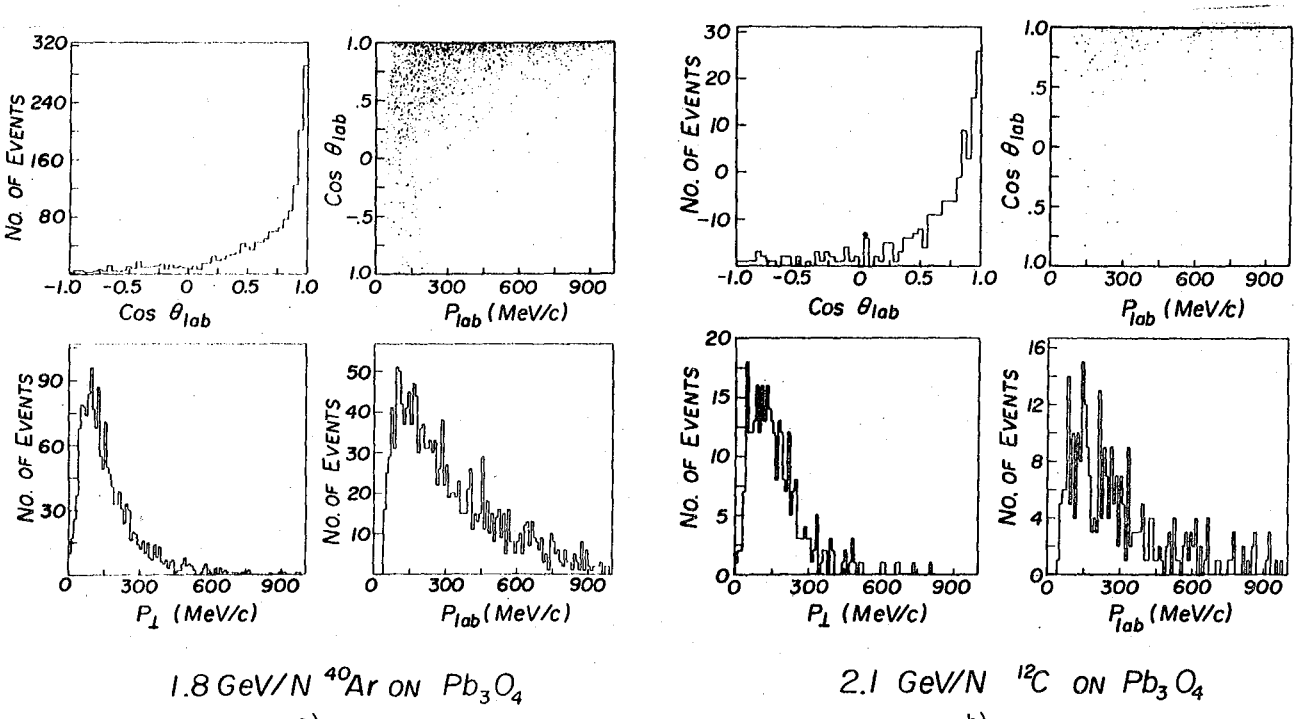

Fig. 41

Momentum and angular distributions of negative pions in the laboratory system for (a) 1.8 GeV/N ^{40}Ar and (b) 2.1 GeV/N ^{12}C incident on Pb_3O_4: cos θ versus total momentum with projections, together with transverse momentum.

Table 1

Projectile	Projectile Energy (GeV/N)	TARGET LiH $\langle N_{\pi^-} \rangle$/int.	LiH $\langle N_{\pi^-} \rangle / \langle N \rangle$	NaF $\langle N_{\pi^-} \rangle$/int.	NaF $\langle N_{\pi^-} \rangle / \langle N \rangle$	BaI_2 $\langle N_{\pi^-} \rangle$/int.	BaI_2 $\langle N_{\pi^-} \rangle / \langle N \rangle$	Pb_3O_4 $\langle N_{\pi^-} \rangle$/int.	Pb_3O_4 $\langle N_{\pi^-} \rangle / \langle N \rangle$
^{40}Ar	0.4	0.043 ± 0.022	0.006 ± 0.003	0.034 ± 0.015	0.003 ± 0.001	0.107 ± 0.019	0.007 ± 0.001	0.099 ± 0.020	0.007 ± 0.001
	0.9	0.31 ± 0.04	0.033 ± 0.004	0.60 ± 0.09	0.044 ± 0.005	0.87 ± 0.09	0.045 ± 0.003	0.92 ± 0.88	0.045 ± 0.003
	1.8	0.97 ± 0.05	0.08 ± 0.003	1.91 ± 0.12	0.104 ± 0.004	3.27 ± 0.18	0.106 ± 0.003	3.27 ± 0.15	0.104 ± 0.002
^{12}C	0.4	0.02 ± 0.01	0.004 ± 0.002	0.038 ± 0.013	0.006 ± 0.002	0.078 ± 0.014	0.010 ± 0.002	0.066 ± 0.014	0.009 ± 0.002
	2.1	0.68 ± 0.07	0.095 ± 0.006	1.03 ± 0.08	0.108 ± 0.006	1.91 ± 0.17	0.110 ± 0.006	1.79 ± 0.16	0.101 ± 0.006

III.A.3. Multiparticle processes in relativistic collisions of nuclei

A number of experiments involving multiparticle final states have been reported to this conference by Baldin[21]. A variety of techniques including a 2m streamer chamber, a propane bubble chamber and a hydrogen bubble chamber have been used. I would like to mention here two interesting results which demonstrate the close relationship between nucleus-nucleus collisions and pp collisions. Fig. 42 shows the dispersion

$$D_- = \sqrt{\langle n_-^2 \rangle - \langle n_- \rangle^2}$$

of the multiplicity distributions of negative particles as a function of $\langle n_- \rangle$ for pp collisions and for α-nucleus interactions at a momentum of 18 GeV/c. The

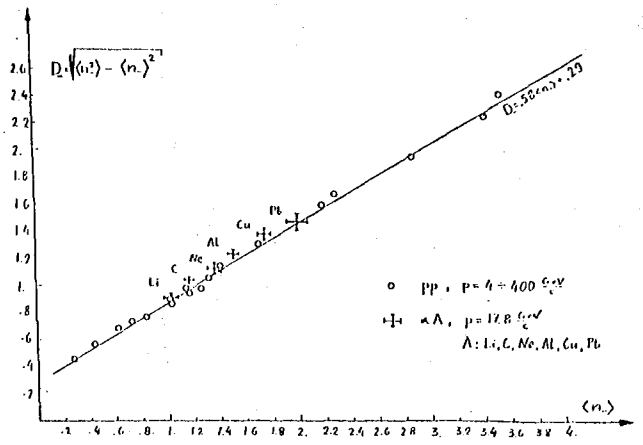

Fig. 42

The dispersion of the multiplicities in nucleus-nucleus collisions, from Baldin[21].

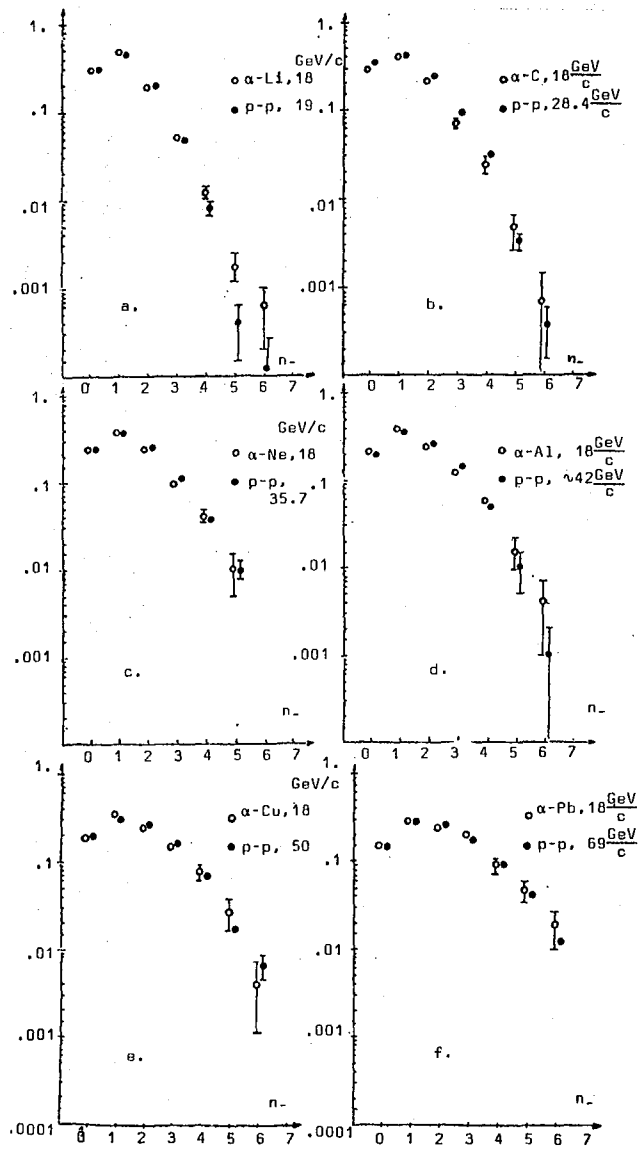

Fig. 43

Comparison of multiplicities for pp and α nucleus interactions, from Baldin[21].

comparison of the multiplicity distributions for pp and α-nucleus interactions is given in Fig. 43 a to f. The data are compared at the energy corresponding to

$$\langle n_- \rangle_{pp} = \langle n_- \rangle_{\alpha A} .$$

These figures well illustrate the assertion that the transition from nucleon-nucleon to nucleus-nucleus is in a certain sense equivalent to the transition of the n-n system to higher energies.

III.A.4. Multiplicities of charged particles

Gosset et al.[12] have reported on measurements of multiplicity of charged particles in High Energy Heavy Ion Reactions. They surrounded their scattering chamber with 80 scintillators. Low energy particles with E/nucleon $\lesssim$ 25 MeV and pions with E < 20 MeV did not reach this multiplicity array. Multiplicities were measured for the various combinations of projectiles

(p, ^{4}He, ^{20}Ne, ^{40}Ar) and targets (^{27}Al, ^{40}Ca, ^{238}U) at incident energies of 0.4 and 1.05 Gev/nucleon. Fig. 44 shows the average multiplicity <M> plotted against

$$R = \frac{Z_{targ} A_{proj}^{2/3} + Z_{proj} A_{targ}^{2/3}}{(A_{proj}^{1/3} + A_{targ}^{1/3})^2}$$

which should be directly related to the total number of participant protons in the target and projectile. They state that according to geometrical assumptions R = <M> if only the participating nucleons contribute to the multiplicity. Their data, which is shown in Fig. 44, indicate a general trend consistent with this hypothesis for projectiles having kinetic energies of .4 GeV/nucleon but not for those with 1.05 GeV/nucleon, which show a higher average multiplicity. They and also Nagamiya et al.[15] find that the differential cross section,

$$\left(\frac{d\sigma}{d\Omega}\right)_{Lab},$$

for a given type of fragment becomes less and less forward peaked with increasing associated multiplicity. It is not yet clear whether this effect is a consequence of kinematic constraints, shadowing or some more esoteric mechanism.

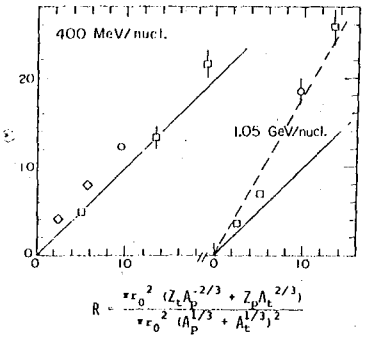

Fig. 44

Average multiplicity <M> versus R defined in the text. Symbols □, o and x refer to U, Ca, and Al targets, respectively. The solid lines correspond to <M> = R. The dashed line is drawn through the 1.05 GeV/N data.

III.B. Theoretical Models of Multiparticle Production

Many of the same theoretical models used to describe single particle spectra also can be used to calculate multiparticle final states. However, uncertainties associated with the underlying assumptions as well as with the caculational approximations and methods have injected a certain "crisis of confidence" in the reliability of the predictions. Macroscopic and microscopic classical and quantum mechanical, relativistic and non-relativistic approaches in various combinations and permutations have been tried in order to determine if "new" phenomena are involved in collisions between fast moving nuclei, but despite all the effort no definitive conclusion can yet be drawn.

It seems to me that we have entered an era where experiments involving multiparticle final states are becoming more and more refined. New techniques (e.g. emulsions in strong magnetic fields, streamer chambers in magnetic fields, etc.) are starting to yield much more detailed kinematic descriptions of these processes. Let us hope the theorists can rise to the occasion and provide us with better calculations.

IV.A. Other Experiments

I would like to briefly mention a number of other experiments whose methods or physics objectives are slightly different from those discussed previously.

IV.A.1 d + d → ^{3}He + n

Bizard et al.[42] at Saclay have studied the energy dependence of the reaction dd → ^{3}He n at total center of mass energies between 3.85 and 4.35 GeV for $0 \leq \theta^{*}_{CM} \leq 60^{o}$. Fig. 45 shows some preliminary results of

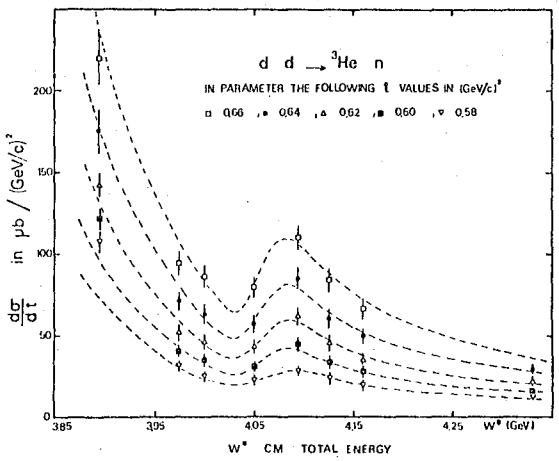

Fig. 45

Cross sections dσ/dt plotted versus total CM energy W* at several t values 0.66, 0.64, 0.62, 0.60 and 0.58 $(GeV/c)^2$.

the energy dependence of dσ/dt at five values of t. The continuous lines are based on a fit of the form:

$$\frac{d\sigma}{dt} = \left[\frac{A}{p^n} + \frac{B(M-M_o)}{(M-M_o)^2 + \frac{\Gamma^2}{4}} \right] e^{\alpha t}$$

with M_o = 1240 MeV and Γ = 70 MeV. They conclude that the data show an s-channel effect that can be interpreted as an excitation of a virtual Δ_{33} resonance responsible for at least part of the reaction mechanisms.

IV.A.2 α + p → α + x

Basini et al.[43] at Saclay have used the reaction α + p → α + x (T = 1/2) to study low mass πN enhancements. As shown in Fig. 46 they see evidence for a narrow bump at M = 1130 MeV/c^2, Γ = 80 MeV/c^2 in both 4.00 and 5.08 GeV/c α's incident. A similar enhancement was observed in an earlier experiment involving the reaction d + p → d + x. In both cases the cross section is strongly peaked forward and decreases rapidly with |t|. They observe a strong mass -|t| slope correlation. All of these features are consistent with a diffractive Deck-type mechanism.

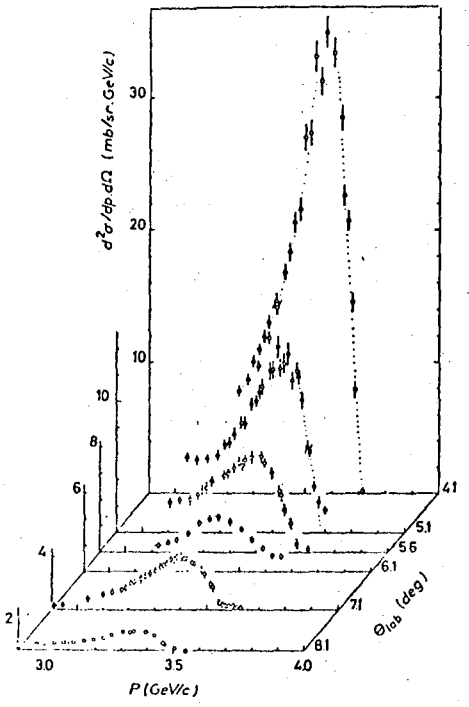

Fig. 46

Momentum spectra of scattered ^{4}He at various angles. The dotted lines on each spectrum are drawn to guide eye. Quoted errors are statistical only. A systematical error of ± 5 % due to normalization uncertainties, must be added.

IV.A.3 Alpha-alpha elastic scattering

α + α elastic cross sections have been reported by Berger et al.[44]. Fig. 47 shows the differential cross section dσ/dt as a function of t for incident momenta of 4.30 and 5.05 GeV/c. Because there are no spin effects to fill in the minima one can determine the ratio of the real to imaginary parts of the NN amplitude. The characteristic diffraction pattern shows minima corresponding to double and triple scattering. The curves are predictions based on two Glauber-type models[45,46].

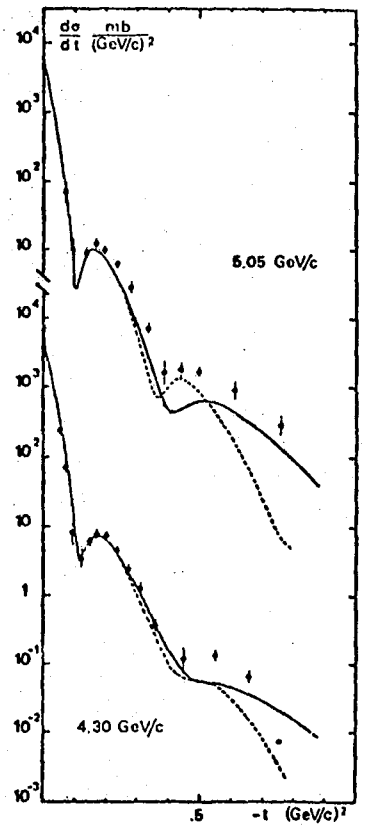

Fig. 47

Elastic αα scattering data for two different incident energies 5.05 GeV/c and 4.30 GeV/c. Solid lines show calculated curves by the Czyz and Maximon model and based on a Gaussian single particle density, and dotted lines by the Malecki and Satta model which introduced correlated pair effects.

IV.A.4 α + p elastic small angle scattering

Measurements of α + p small angle elastic differential cross sections have been made at Dubna at energies of 1.75 to 4.13 GeV/nucleon. The results were used to determine the ratio

$$\alpha = \frac{\mathrm{Im}f}{\mathrm{Re}f}$$

of the scattering amplitude f. Fig. 48 shows the energy dependence of α. The curve shows results of a calculation based on dispersion relations. The discrepancy at the highest energies is probably not significant because of uncertainties in the theoretical calculations.

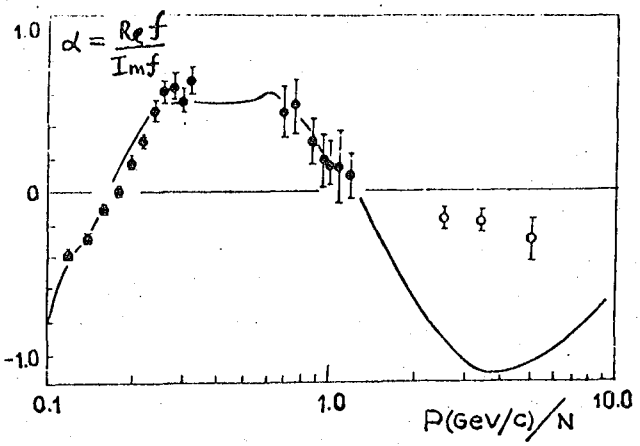

Fig. 48

The ratio of real to imaginary part for the elastic pα amplitude from Coulomb interference experiments, Baldin[21].

In the domain of light nuclei at very high energy; dd interactions have been studied at the CERN ISR[47]. (Those of you interested in nuclei at these very high energies may be pleased to know that it is possible in principle, and without extensive modifications, to inject other light nuclei into the ISR or to accelerate them in the SPS.) The ISR dd experiment was mainly directed toward studying diffractive dissociation of neutrons on deuterons. An example of the type of results obtained with the Split Field Magnet detector is shown in Fig. 49. In addition to the broad low effective $\pi^- p$ mass peak there is considerable production of a narrow peak at ∿ 1690 MeV. In the course of this experiment they also measured differential cross sections for pd and dd elastic scattering.

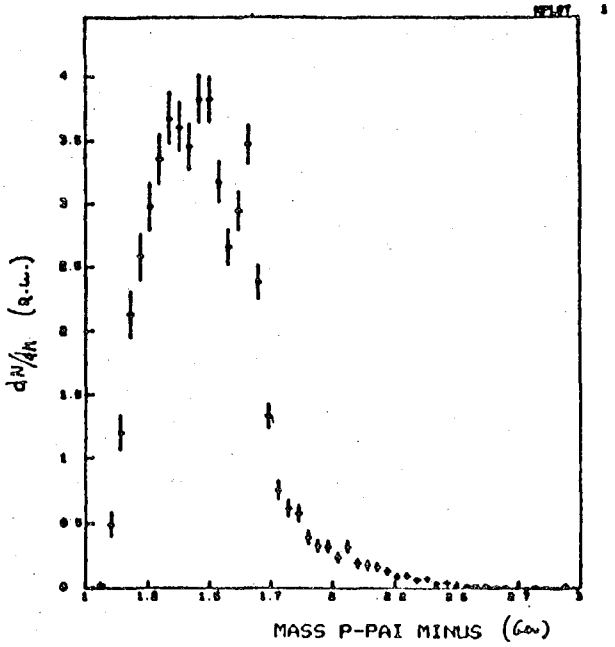

Fig. 49

Effective mass spectrum of $p\pi^-$ obtained in dd reactions at ISR, CERN.

V. Summary and Outlook

Research involving high energy nuclei has grown impressively during the past few years. The experiments have become both much more extensive, covering much broader kinematical domains, and more refined. I have tried by presenting some examples to convey a general picture of present activities in this field of study and thereby also to illustrate the underlying physics. I have perhaps over-emphasized experimental results near the kinematic boundaries - the shaded regions of Fig. 1 - but I think these regions are of particular interest because they give new information about the short-distance behavior of nuclear wave functions. The variety of theoretical approaches to explain such phenomena is great, but basically they are all attempts to describe this short-distance behavior. There is still no theory which explains all the observations completely, but nevertheless very significant progress has been made in our theoretical understanding of these phenomena. The very extensive measurements of single particle inclusive spectra as a function of bombarding energy, projectile type, target, fragment type and momentum have started to show certain regularities and patterns which in turn reflect the dominant interaction mechanisms.

The present situation with respect to "new" phenomena is still murky. The problem here is that we do not understand ordinary nuclear physics well enough, so unless the observed effects are really startling we have great difficutly resolving the extra-ordinary from the ordinary. In my perhaps overly conservative opinion there is not yet any convinving evidence that nuclear shocks, pion condensates or other "abnormal" phenomena have been observed. On the other hand the experiments do not rule out the possibility that such effects are indeed taking place, and it seems clear that this area of research will continue to be actively pursued.

The study of multiparticle states is still at its infancy and here both experimental and theoretical refinements are needed. The relation between multiparticle production in hadron-nucleus and nucleus-nucleus interactions at high energies is just starting to be established.

What about the future? Many fascinating problems remain to be resolved, and it will be a challenge to both experimenters and theorists to come to practical grips with them. Technically the outlook is promising. The accelerators continue to improve in performance both in the intensity and quality of the available beams and the variety of projectiles available. A new generation of spectrometers and detectors are coming into operation and promise to yield data of even higher quality.

Especially in the field of multiparticle final states we can expect significant developments in the next few years.

It is fun to speculate about such fascinating topics as the space-time structure of nuclear interactions at high energy, the quark structure of nuclei (e.g. is the short range repulsion between nucleons simply a consequence of the Pauli Principle applied to the quark constituents?), the role of nuclei in the "new" spectroscopy of charm and color. Perhaps experiments with nuclei at sufficiently high energies can give us some new insights into these and other questions.

I would like to express my thanks to Profs. L. Bertocchi, J. Hüfner, Drs. L. Anderson, S. Nissen-Meyer, S. Nagamiya and Ms.H.Holtz for their cooperation and help in preparing this report.

I acknowledge with thanks the hospitality of the Max-Planck-Institute for Physics in Munich and the support of the Alexander von Humboldt Foundation.

References

1) W. Busza, "Review of Experimental Data on Hadron-Nucleus Collisions at High Energies", invited talk given at the VIIth International Colloquium on Multiparticle Reactions at Tutzing, Tutzing (June, 1976)

2) C. Halliwell, "Production on Nuclei", invited talk given at the VIIIth International Colloquium on Multiparticle Reactions at Strasbourg, Strasbourg (June, 1977)

3) J. Otterlund, "Multiparticle Production on Nuclei at Very High Energies", invited talk given at the Topical Meeting on Multiparticle Production on Nuclei, Trieste (June, 1976)

4) T.D. Lee, Ref.Mod.Phys. 47 (1975) 267

5) A.B. Migdal, N.A. Kirichenko, and G.A. Sorokin, Phys.Rev.Letters 50B (1974) 411

6) H.G. Baumgardt, J.U. Schott, Y. Sakamoto, E. Schopper, H. Stöcker, J. Hofmann, W. Scheid, and W. Greiner, Z.Phys. A273 (1975) 359

7) J. Papp, J. Jaros, L. Schroeder, J. Staples, H. Steiner, A. Wagner, and J. Wiss, Phys.Rev.Lett. 34 (1975) 601, and, to be published J. Papp, LBL-3633, Berkeley (1975), Ph.D. Thesis (unpublished)

8) L. Anderson, Berkeley (1977), Ph.D. Thesis, in preparation

9) D.E. Greiner, P.J. Lindstrom, H.H. Heckman, Bruce Cork, and F.S. Beiser, Phys.Rev.Lett. 35 (1975) 152

10) M. Gazzaly, Berkeley (1977), Ph.D. Thesis, in preparation

11) A.M. Zebelman, A.M. Poskanzer, J.D. Bowman, R.G. Sextro, and V.E. Viola Jr., Phys.Rev. 11C, 1280

12) J. Gosset, H.H. Gutbrod, W.G. Meyer, A.M. Poskanzer, A. Sandoval, R. Stock, and G.D. Westfall, LBL-5820, May 1977, submitted to Phys.Rev. C and contributed paper, this conference.

13) H.J. Crawford, P.B. Price, J. Stevenson, and Lance W. Wilson, Phys.Rev.Lett. 34 (1975) 329

14) A.M. Poskanzer, R.G. Sextro, A.M. Zebelman, H.H. Gutbrod, A. Sandoval, and R. Stock, Phys.Rev. Lett. 35 (1975) 1701

15) S. Nagamiya, I. Taniahta, S.R. Schnetzler, W. Brückner, L. Anderson, G. Shapiro, H. Steiner, and O. Chamberlain, to be published

16) A.M. Baldin, S.B. Gerasimov, N. Ghiordanescu, V.N. Zubarev, L.K. Ivanova, A.D. Kirillov, V.A. Kuznetzov, N.S. Moroz, V.B. Radomanov, V.N. Ramznin, V.S. Stavinsky, M.I. Yatsuta, Yad.Fiz. 18 (1973) 79

17) G.D. Westfall, J. Gosset, P.J. Johansen, A.M. Poskanzer, W.G. Meyer, H.H. Gutbrod, A. Sandoval, and R. Stock Phys.Rev.Lett. 37 (1976) 1202

18) J.W. Cronin et al., Phys.Rev. D11 (1975) 3105

19) Yu.D. Bayukov, V.I. Efremenko, V.B. Fedorov, V.B. Gavrilov, G.A. Leksin, V.S. Pavlov, D.A. Suchkov, B.B. Shvartsman, and Yu.M. Zaitsev, ITEP Preprint, ITEP-49 (1977)

20) Yu.E. Belikov, A.E. Bukley, V.B. Cavrilov, M.M. Kats, L.N. Kondratiev, G.A. Leksin, V.S. Pavlov, N.N. Pomelov, V.Yu. Rusinov, and B.A. Yeshov, contributed paper H-25 this conference

21) A.M. Baldin, contributed paper I-22 this conference

22) H. Brody, S. Frankel, W. Frati, D. Yang, C.F. Perdrisat, J.C. Comiso, K.O.H. Ziock, Univ. of Pennsylvania, Preprint UPR-0046N (1977)

23) S. Frankel, Phys.Rev.Lett. 38 (1977) 1338

24) I.A. Schmidt and R. Blankenbecler, Phys.Rev. 15D (1977) 3321

25) V.V. Burov, V.K. Lukyanov, A.I. Titov, Phys.Lett. 67B (1977) 46, and contributed papers H-15, H-22 this conference

26) A.M. Baldin et al. Yad.Fiz. 18 (1973) 79

27) T. Fujita, Phys.Rev.Lett. 39 (1977) 174

28) S. Frankel, W. Frati, D. van Dyck, R. Werbeck, V. Highland, Phys.Rev. Lett. 36 (1976) 642

29) A. Dar, Proceedings of the Meeting on Nuclear Production at Very High Energies, S.A. Azimov, ed., Trieste, June, 1976

30) H.H. Gutbrod, A. Sandoval, P.J. Johansen, A.M. Poskanzer, J. Gosset, W.G. Meyer, G.D. Westfall, and R. Stock, Phys.Rev.Lett. 37 (1976) 1202

31) S.T. Butler, and C.A. Pearson, Phys.Rev.Lett. 7 (1961) 69, Phys.Lett. 1 (1962) 77, and Phys.Rev. 129 (1963) 836

32) A.A. Amsden, F.N. Harlow, and J.R. Nix, Phys.Rev. 15C (1977) 2059

33) A. Bialas, M. Bleszynski, and W. Czyz, Nucl.Phys. B111 (1976) 461

34) W.J. Swiatecki, unpublished LBL-internal report (1976)

35) A.M. Poskanzer, R.G. Sextro, A.M. Zebelman, H.H. Gutbrod, A. Sandoval, and R. Stock, Phys.Rev. Lett. 35 (1975) 1701

36) B. Jakobsson, R. Kullberg, and I. Otterlund, Nucl.Phys. A276 (1977) 523

37) V.D. Toneev, K.K. Gudima, contributed paper I-24 this conference

38) P.J. McNulty, G.E. Farrel, R.C. Filz, S. Schimmering, and K.G. Vosburgh, Phys.Rev.Lett. 38 (1977) 1519

39) G.F. Bertsch, Phys.Rev. 15C (1977) 713

40) Y. Kitazoe, M. Sano, and H. Tok, Lett. al Nuovo Cimento 13(1975) 139; Y. Kitazoe, and M. Sano, Lett. al Nuovo Cimento 14 (1975) 400, 407

41) S.Y. Fung, W. Gorn, G.P. Kiernan, F.F. Liu, J.J. Lu, Y.T. Oh, J. Ozawa, R.T. Poe, L. Schroeder, H. Steiner, submitted to Phys.Rev.Lett.

42) G. Bizaro, J.L. Laville, C. LeBrun, J.F. Lecolley, F. Lefebvres, A. Osmont, R. Regimbart, J.C. Steckmeyer, J. Berger, J. Duflo, L. Goldzahl, F. Plouin, J. Oostens, F.L. Fabbri, P. Picozza, L. Satta, contributed paper I-6 this conference

43) G. Basini, J. Berger, G. Bizard, J. Duflo, F.L. Fabbri, L. Goldzahl, C. LeBrun, J. Oostens, P. Picozza, F. Plouin, L. Satta, M. van den Bossche, and L. Vu Hai, Frascati Preprint LNF-77/21 (P) (1977) (unpublished)

44) J. Berger, J. Duflo, L. Goldzahl, F. Plouin, J. Oostens, F.L. Fabbri, P. Picozza, L. Satta, G. Bizard, F. Lefebvres, J.C. Steckmeyer, T. Bauer, D. Legrand, and M. Matoba, contributed paper I-1 this conference

45) W. Czyz and L.C. Maximon, Ann.Phys. (N.Y.), 52 (1969) 59

46) A. Malecki, and L. Satta, Frascati Internal Report LVL 77/36 (unpublished)

47) M. Cavalli-Sforza, C. Conta, M. Fraternali, G. Goggli, M. Livan, G.C. Mantovani, F. Pastore, A. Rinoldi, B. Rossini, private communication

DISCUSSION

A.M. BALDIN
We have not had a chance to report to this conference a large number of results on relativistic nuclear interactions obtained by people from JINR Dubna, ITEP Moscow and Erevan, but fortunately the viewpoint of the Berkeley group at present almost coincides with that expressed by us at Santa Fé, and was presented very clearly by Dr. Steiner. In particular, I mean: (1) Universal dependences of one-particle distributions $\rho \propto e^{-T/T_0}$ with $T_0 \approx 66 \div 70$ MeV; (2) A-dependences; (3) Difficulty of explanation of the cumulative effect by Fermi motion.

The model of cumulative effects has been supported and developed by Prof. Dar et al. They were able to explain a large amount of experimental information, and predict new phenomena. Data presented by me at the workshop does not contradict the cumulative model, but is supporting it. Such a simple model could not pretend to be an explanation of everything. You can find some results in abstracts of papers presented at this conference.

H. STEINER
I did not have time to go into details of models. The point I want to come back to and emphasize is that we are talking about short distance behaviour of nuclear wave functions. The cumulative effect is one way of describing that behaviour which seems to work in a lot of processes. For example, I think that the model of quasi two-body scaling, which does not have really any physical basis except to say that there is a high momentum tail, also explains the data. The model of Schmidt and Blankenbecler, which is an independent particle model, does quite well in explaining some data, not so well in explaining other. Obviously, there is a close connection between high Fermi momentum and high local density, and I think I would try to make the point that the different descriptions may have the same underlying physics.

A. DAR
Well, I have to disagree with what you are saying. You can express everything in terms of density distributions. You can Fourier transform any wave-function into momentum space and call it Fermi motion. The question is, is it the conventional Fermi motion or something very unusual? I am very sorry that the Dubna group could not present in a short period of time all their data because there is more and more accumulating evidence not only at a few GeV per nucleon but at 400 GeV that there are many phenomena that cannot be explained by conventional Fermi motion. Of course you can plug in momentum distributions that will fit specific experiments, but the collective models are a very convenient way to describe the data, especially at energies higher than those at Berkeley.

H. STEINER
I agree with your statements. I also believe that conventional Fermi motion where you just assume some Gaussian does not do it. You have to add something, and that is characteristic of short distances.

This report was done with support from the United States Energy Research and Development Administration. Any conclusions or opinions expressed in this report represent solely those of the author(s) and not necessarily those of The Regents of the University of California, the Lawrence Berkeley Laboratory or the United States Energy Research and Development Administration.